Technical Report No. TRL-101

THE MEASUREMENT OF TURBULENCE WITH THE LASER DOPPLER ANEMOMETER*

by

P. Buchhave**, W. K. George, Jr.,
and John L. Lumley***

Turbulence Research Laboratory
Faculty of Engineering and Applied Sciences
State University of New York at Buffalo
Buffalo, New York 14214

* Prepared for publication in Annual Review of Fluid Mechanics, Annual Reviews, Inc., Palo Alto, California 94306 (Van Dyke and Wehausen, coeditors).

** On leave from DISA Elektronik, A/S, Copenhagen, Denmark.

***Sibley School of Mechanical & Aerospace Engineering,
Cornell University, Ithaca, New York 14853

ACKNOWLEDGEMENTS

William K. George and Preben Buchhave acknowledge the support of the U. S. National Science Foundation, Meterology Program under Grant Number ATM 76-02157 and the Fluid Mechanics Program under Grant ENG 76-17466.

Preben Buchhave acknowledges the support of the Danish Natural Science Research Council and the Danish Council for Scientific and Industrial Research.

John L. Lumley is pleased to acknowledge several helpful discussions with S. Liebovich and the support of the U. S. National Science Foundation, Meterology Program under Grant Number ATM 77-22903, the U. S. Office of Naval Research, Fluid Dynamics Branch and the U. S. Air Force Office of Scientific Research.

The authors are grateful to Eileen Graber for typing the manuscript and to Bonita Webb for assisting with the literature search.

INDEX

1. INTRODUCTION

1.1 The Laser Doppler Method

The laser Doppler Anemometer (the LDA in the following) is an instrument for fluid flow research which has the potential of allowing local time resolved measurements of fluid velocity without disturbing the fluid phenomenon under investigation. However, as in the case of its main competitor in the field, the hot-wire anemometer, the application of the LDA to turbulence measurements is not trivial and the problems (and the challenges) facing the experimenter grow with increasing levels of the turbulent fluctuations. This article reviews the status of turbulence measurements with the LDA and outlines the achievements of the past few years and some of the remaining problems. The article will deal with only those methods allowing time resolved measurements of the velocity, and thus we shall not treat such signal processing methods as spectrum analysis of the Doppler signal or time-averaged photon correlation.

The laser Doppler method is based on the measurement of the Doppler shift of laser light scattered from small particles carried along with the fluid. Due to the motion of the particles the frequency of the scattered light will be shifted by an amount $\omega_D = \underline{K} \cdot \underline{u}$, where $\underline{K} = \underline{K}_s - \underline{K}_i$ is the difference between the wave vector of the scattered and incident light respectively and $\underline{u} = (u,v,w)$ is the velocity of the medium (Fig. 1-1). The stability and spatial coherence of the gas laser output allow the light to be focused to a small spot within the fluid. Excellent monographs now exist on the basic theory of the LDA and the reader is referred to these for further information (Durst, Melling and Whitelaw (1976), Durrani and Greated (1977)). For the detection of the frequency shift, the optical heterodyning or light-beating effect of a square law photodetector is utilized. The scattered light is mixed on the surface of the photodetector with a reference beam derived directly from the laser or with light scattered from another incident beam. Figure 1-2 shows the optical

arrangement, which is almost exclusively used today, and also serves to define the basic optical parameters.

The function of the optical system is partly to direct and focus the incident beams to a small volume within the flow field, and partly to collect the scattered light from this volume while simultaneously discriminating against ambient light and light scattered from regions outside the volume. For clarity it is desirable to distinguish between the region of space defined by the intersection of the two incident beams, which we shall designate the probe volume, and the region in space from which Doppler signals are detected, which we shall designate the measuring volume. The measuring volume is more difficult to define than the probe volume since it depends on the field of view of the detector, the overall gain in the system, and even on the method of signal processing. The probe volume is usually defined by the $1/e^2$ - boundary of the modulation depth of the interference pattern existing in the beam intersection region. With Gaussian laser beams the probe volume is an ellipsoid, and we have the familiar expression for the probe volume dimensions in terms of the half-axes of the ellipsoid in the coordinate system defined in Figure 1-2 (a,b, and c) or the standard deviation of the Gaussian intensity distribution (σ_x, σ_y and σ_z):

$$2a = 4\sigma_x = \frac{d_1}{\cos(\theta/2)} \tag{1.1.1a}$$

$$2b = 4\sigma_y = d_1 \tag{1.1.1b}$$

$$2c = 4\sigma_z = \frac{d_1}{\sin(\theta/2)} \tag{1.1.1c}$$

where d_1, the beam waist of the focused laser beam in the measuring volume, may be expressed as

$$d_1 = \frac{4}{\pi} \frac{\lambda}{\Delta\theta} \tag{1.1.2}$$

and where $\Delta\theta$ is the beam convergence angle of the focused beam, and λ the

wave length of the laser light.

The photodetector responds to the square of the total light field incident at each point of the detector surface, $di \propto |E_t|^2$, where $E_t = E_1 + E_2$, and E_1 and E_2 represent the scalar field strength at the detector surface of the scattered light and the reference beam in the reference beam mode or the two scattered beams in the dual-scattered beam mode. The resulting photocurrent is the sum of contributions from each point of the detector surface:

$$i \propto \int_{A_d} |E_t|^2 dA = \int_{A_d} |E_1|^2 dA + \int_{A_d} |E_2|^2 dA + \int_{A_d} (E_1 E_2^* + E_1^* E_2) dA \qquad (1.1.3)$$

where A_d is the total detector area.

In case of a single particle at location $\underline{x}_p(t)$ the resulting photocurrent may be written as

$$i_{sp}(t) = i_1(t) + i_2(t) + 2\sqrt{i_1(t)\, i_2(t)} \cos [\omega_D t + \phi_p], \qquad (1.1.4)$$

where $i_1(t)$ and $i_2(t)$ are the currents which would be caused by each incident beam acting alone and where the Doppler frequency ω_D is given by

$$\omega_D = [4\pi\, u_p/2] \sin (\theta/2). \qquad (1.1.5)$$

u_p is the x-component of the instantaneous particle velocity $\underline{u}_p$ and ϕ_p is a constant phase term depending on the initial location of the particle. The a.c. part of the signal can be written

$$i_{sp,ac}(t) = I\, w[\underline{x}_p(t)] \cos [\omega_D t + \phi_p], \qquad (1.1.6)$$

where $w(\underline{x}) = 2\sqrt{i_1(\underline{x})\, i_2(\underline{x})}$ may be regarded as a weight function describing the intensity of the modulated part of the detector signal received from space location $\underline{x}$, and I includes the scattering characteristics of the particle.

In general, when many particles are present simultaneously in the measuring volume, the Doppler signal will consist of a slowly varying part (the d.c. part or pedestal) and a higher frequency term (the a.c. or Doppler modulated term):

$$i(t) = i_1(t) + i_2(t) + 2\sqrt{i_1(t)i_2(t)}\cos[\omega_D t + \phi(t)] \qquad (1.1.7)$$

where now

$$\omega_D = [4\pi u_o/2]\sin(\theta/2). \qquad (1.1.8)$$

$i_1(t)$, $i_2(t)$ and $\phi(t)$ are now randomly fluctuating quantities resulting from the superposition at the detector surface of the scattered optical fields from all illuminated particles. Normally, there are many interference fringes within the measuring volume, in which case $i_1(t)$, $i_2(t)$ and $\phi(t)$ are slowly varying relative to the cosine term. $\underline{u}_o = (u_o, v_o, w_o)$ represents the velocity of the fluid in the measuring volume. The exact definition of $\underline{u}_o$ depends on the circumstances of the measurement, and a further discussion is deferred to the description of particular cases later in this article.

From eqs. (1.1.5) and (1.1.8) we see that the LDA instrument measures the x-component of the instantaneous velocity $\underline{u}_o$; the instrument is totally insensitive to the other velocity components v_o and w_o. However, the particle transit time or residence time is determined by the magnitude of the total velocity vector. As we shall discuss in sections 2 and 3, the properties of the Doppler signal and the noise level and accuracy of the system as a whole are determined by the magnitude and direction of the total velocity vector relative to the orientation of the optical beams. Furthermore, it should be noted that the relation between the Doppler frequency and the velocity u_o is linear; thus, calibration is limited to the determination of the coefficient of proportionality given by the laser wavelength λ and the beam intersection angle θ. Complete characterization of the turbulent velocity field requires simultaneous determination of all three velocity components. For practical and economical reasons, however, many investigations are carried out with a one-component system which in some cases creates special problems because of the unknown magnitude and direction of $\underline{u}_o$.

The properties of the Doppler signal and thus the proper method of

signal processing depends strongly on the number of particles present in the measuring volume and the mode of operation of the detector optics, Drain (1972),Lading (1973), Hanson (1974). If the probability that two or more particles are present simultaneously in the measuring volume is negligible, the best signal-to-noise ratio of the Doppler signal is obtained in the so-called incoherent detection mode, in which a large detector aperture is used to collect a maximum of scattered light from a single particle. The detector optics is fully able to resolve the interference fringe pattern existing in the probe volume (this mode of operation is often referred to as the fringe mode). If many particles simultaneously occupy the measuring volume, the photocurrent contributions from the individual particles add incoherently at the detector surface, $i_d(t) = \Sigma\, i_n(t)$, where $i_n(t)$ is the detector current caused by each individual particle independent of the others. However, in the many-particle case a better signal-to-noise ratio can be obtained using the coherent detection mode. In this mode the receiver aperture is kept so small that the scattered light from all particles add coherently on the detector surface: $i_d(t) \propto (\Sigma\, E_n(t))^2$. In the coherent detection mode the signal strength can be enhanced by using a strong reference beam and the signal-to-noise ratio improved with the addition of more particles, whereas the signal-to-noise ratio is independent of particle number in the incoherent detection mode.

The type of signal encountered in actual measurements depends on the fluid and the type and amount of seeding material added. In order to control the characteristics of the particle motion it is desirable to work only with monodisperse scattering particles uniformly distributed in the fluid. When this is not possible the experimenter can in most cases exert a certain amount of control over the size of particles contributing to the signal accepted by the processor by adjusting signal gain and in some cases by setting levels for the rejection of very low or very high amplitude signals. Continuous, many

particle signals are most often encountered in measurements in liquids, whereas Doppler signals from measurements in gases are often of the single burst type. In this article we do not intend to enter the subject of light scattering from small particles or the questions concerning the proper seeding methods or materials, but again refer the reader to the monographs on LDA measurements and the articles by Farmer (1972), Durst and Eliasson (1976) and Adrian and Orloff (1977), where these problems are discussed and references to specialized papers on the subject may be found.

1.2 Physical Parameters Affecting the Doppler Signal

As indicated above the LDA responds to the component of fluid velocity normal to the interference fringe planes in the probe volume. The actual physical process underlying the laser Doppler method can be described as a measurement of the phase difference of two optical waves scattered by small particles in the probe volume. The time rate of change of this phase difference can be interpreted as a measure of the suitably defined fluid velocity relative to the interference fringe planes in the probe volume. Evidently this interpretation requires that the particles follow the fluid motion with negligible slip due to fluid shear or acceleration. This aspect of the problem will be taken up in Section 5; in the meantime it will be assumed that the particles follow the fluid motion exactly. The only other physical parameter of the fluid directly affecting the phase of the scattered light is the refractive index. Index of refraction variations may cause small random shifts in the phase of the optical beams and thereby in the location of the interference fringe planes. Larger optical inhomogeneities may cause the measuring volume to move about randomly or cause the beams to miss each other resulting in a loss of signal or a reduced signal-to-noise ratio. Optical index fluctuations are primarily a result of density fluctuations (in turn caused by pressure or temperature fluctuations) or in the case of

turbulent mixing or combustion,a result of concentration fluctuations. The effect of optical index fluctuations on the spectral properties of the Doppler signal is treated in Section 4. Meanwhile we shall consider the fluid to be of constant density and refractive index.

In addition,the signal phase is influenced by electronic noise from various sources of which the most important are the detector shot noise and the thermal noise in the input circuit to the signal processor. Usually it is possible to operate the system in such a way that the detector shot noise is dominant (shot noise limited signal), and in this case the signal-to-noise ratio is directly proportional to the power of the incident laser beams.

In the following discussion it will be convenient to introduce the concept of the "ideal LDA" in which shot noise and thermal electronic noise may be considered negligible, and where the optical system may be considered perfect. A perfect optical system would be one in which no optical aberrations or alignment errors exist, so that the interference fringe system is undistorted and at a fixed location in space. For the purpose of investigating the inherent properties of the LDA as an instrument for turbulence measurements, we shall assume an ideal LDA for the remainder of this paper; the influence of noise and optical distortions will not be considered.

1.3 Signal Processor Operation

In addition to the above considerations, two other main factors determine the performance of the LDA in turbulence measurements: First, the type or appearance of the Doppler signal, i.e., whether the signal may be considered "quasi-continuous",or whether it consists of single bursts interspersed with periods of low power shot noise. Second, the type of signal processor employed, and even to a certain degree, the mode of operation of the signal processor.

Details of the principles and modes of operation of the various types of

LDA signal processors will not be described here; the reader is referred to the ample literature on the subject. For our discussion of turbulence measurements it suffices for the moment to distinguish between two distinct operating modes: one, the frequency demodulator type (of which the frequency tracker may be taken as the prime example) operating on continuous signals, and two, the burst processor, which essentially measures the time for a particle traversal through the measuring volume or through some finite length within the measuring volume. An example of the last kind of processor is the burst counter or LDA-counter, which measures the time for an integer number of zero-crossings of a high-pass filtered Doppler burst. Other systems operating in the burst mode have been developed, e.g. the filter bank (Baker and Wigley (1967))and the burst correlator (Fog (1976)).

It is however, important to note that many of these processors may operate in either the continuous, tracking mode or the burst mode depending on the choice of parameters such as signal level and bandwidth. As an example, the frequency tracker is normally applied to quasi-continuous signals. However, most trackers have a distinct minimum operational input signal level below which the tracking loop will be broken and the instrument kept in a hold-mode (drop-out protection). If the input signal is lowered sufficiently, so that only the highest peaks of the fluctuating envelope are allowed to exceed the drop-out level, the tracker will operate in a single burst-detection mode. If the burst frequency appears within the instrument's "capture range", it will acquire lock and track each burst, but remain in drop-out condition in the time intervals between bursts. Conversely, a typical burst-type instrument as the LDA-counter may operate in a continuous mode on a continuous signal and even provide an analog output through a D/A-converter.

With these qualifications in mind we shall in the following consider in more detail the operation of the tracker as a typical example of a continuous LDA-signal processor providing essentially a continuous analog output and

the operation of the LDA-counter as an example of the burst processor providing one digital velocity sample per burst.

2. THE CONTINUOUS LDA

2.1 The Doppler Current

The statistical properties of continuous, many-particle Doppler signals can now be regarded as well understood. The detector current was initially treated as a superposition of random phase wave packets(Greated & Durrani (1971)) and the methods of analysis of noise in FM demodulators applied to derive the statistical properties of the amplitude and phase fluctuations of the envelope of signals from steady flows. Edwards et al (1971) applied the methods of light-beating spectroscopy to the optical spectrum and the resulting photo-current and derived expressions for the spectral properties of the detector current in steady, non-uniform flow. They showed the spectrum from a Gaussian measuring volume to be Gaussian with a half-width inversely proportional to the diameter of the measuring volume while the spectrum in non-uniform flow was shown to be skewed and broadened as a result of gradients within the measuring volume.

George and Lumley utilized the fact that the turbulent velocity fluctuations and the particle distribution are statistically independent to create a framework for incorporating both the flow field statistics and the fluctuations caused by the random scattering center positions in a unified treatment George and Lumley (1973)*. Since this is the only approach which has led to explicit results for the instantaneous Doppler signal in turbulent flow, it will be followed below.

It is convenient to represent the Doppler current by the following expression

$$i(t)= \frac{1}{N(t)}\int i_{sp}(\underline{a},t)\, g(\underline{a})d\underline{a} \qquad (2.1)$$

where $i_{sp}(\underline{a},t)$ is the time dependent current generated by the particle that was at $\underline{a}$ at $t = o$, where $g(\underline{a})$ is a function which accounts for the presence (or absence) of a particle at $\underline{a}$, and where $N(t)$ is the instantaneous number

* hereafter referred to as reference I.

of particles in the volume. This expression is exactly equivalent to one in which the current is represented as the sum of the currents generated by the particles in the volume.

The current generated by a single particle passing through the scattering volume can be represented as

$$i_{sp}(\underline{a},t) = I\, w(\underline{x}) \cos \underline{K} \cdot \underline{x} \tag{2.1.2}$$

where $\underline{K}$ is the previously defined scattering wavevector, $\underline{x} = \underline{x}(\underline{a},t)$ is the position of the particle which started at $\underline{a}$, and $Iw(\underline{x})$ is the envelope of the current. The function $w(\underline{x})$ is defined so that $w(0) = 1$ and can be taken to specify the spatial extent of the scattering volume by defining

$$V \equiv \int w(\underline{x}) d^3\underline{x} \tag{2.1.3}$$

A consequence of this is that the instantaneous number of particles in the volume is

$$N(t) = \int w(\underline{x}[\underline{a},t]) \; g(\underline{a}) \; d^3\underline{a} \tag{2.1.4}$$

If we operate only on the current generated by individual particles (eqn. 2.1.2), we can in a straight-forward manner obtain the velocity information from the time dependent phase since

$$\theta(t) = \underline{K} \cdot \underline{x} = \underline{K} \cdot \left[\underline{a} + \int_0^t \underline{u}(\underline{a},t')dt'\right] \tag{2.1.5}$$

and

$$\dot{\theta}(t) = \underline{K} \cdot \underline{u}(\underline{a},t') \tag{2.1.6}$$

This attractive possibility will be explored later when we consider burst counters. Unfortunately, for the continuous (many particle) case considered here things are more complicated.

2.2 The Velocity Measured by the Continuous LDA

Ideally one would like to begin from the phase of the Doppler current and identify a portion of the phase as the velocity signal. Unfortunately, because of the random character of the fluctuations in phase and their many sources, there is no straight-forward way to accomplish this. That this is

so is readily obvious by substituting equations 2.1.2 and 2.1.5 into equation 2.1.1 and observing that since $w(\underline{x})$ is, in effect, time dependent because of the particle's motion, it is not possible to directly separate the velocity dependent part of the phase.

George and Lumley (1973) recognized the apparent impossibility of this approach and proposed instead that for the continuous LDA an effective velocity be defined as an average over the volume of the velocities of the particles present. Formally this can be written as

$$u_o(t) = \frac{1}{N(t)V} \int u(\underline{a},t)\, w(\underline{x}[\underline{a},t])\, g(\underline{a})\, d^3\underline{a} \qquad (2.2.1)$$

This approach was particularly useful for the cases where the flow could be assumed incompressible, and the particles were statistically uniformly distributed throughout space. With several additional local assumptions it was possible to show that the statistics of this effective velocity could be separated from the other sources of random phase fluctuations and was therefore an appropriate (although possibly non-unique) choice for the measured velocity.

The relation of u_o to the Eulerian velocity at the center of the volume can be computed from the following relationships:

$$U_o = \frac{1}{V} \int \overline{u(\underline{x},t)}\, w(\underline{x}) d^3\underline{x} \qquad (2.2.2)$$

$$\overline{(u_o - U_o)^2} = \frac{1}{NV} \int w^2(\underline{x}) \overline{u'^2(\underline{x})}\, d^3\underline{x}$$

$$+ \frac{1}{V^2} \iint w(\underline{x})\, w(\underline{x}')\, \overline{u'(x)u'(x')}\, d^3\underline{x}\, d^3\underline{x}' \qquad (2.2.3)$$

The overbar is used to represent the ensemble average, primes are taken to represent fluctuating values, and capital letters are hereafter used to denote mean values unless otherwise noted. In most cases of interest for the continuous LDA, the expected number of particles in the volume, N, is large and the first term in equation (2.2.3) can be neglected.

From equation (2.2.2), the effect of the spatial averaging on measurements of the mean velocity can be shown directly to depend (to first order) on the curvature of the profile. This was first pointed out by Edwards et al (1971) who treated only laminar flow. The results are seldom important for turbulence measurement since mean profile curvature effects are relatively less important than for laminar flow.

George and Lumley (1973) calculated the effect of the spatial averaging in equation (2.2.3) on the measured spectrum in a homogeneous, isotropic turbulent flow for an ideal Gaussian scattering volume for which

$$w(\underline{x}) = \exp\left[-\left(\frac{x^2}{2\sigma_1^2} + \frac{y^2}{2\sigma_2^2} + \frac{z^2}{2\sigma_3^2}\right)\right] \qquad (2.2.4)$$

Using Taylor's hypothesis to convert temporal variations to spatial variations (i.e. converting frequency to wavenumber by $\omega = kU$) and defining a transfer function as

$$T(k) = \frac{\text{Measured spectrum}}{\text{True spectrum}} = \frac{Fm(k)}{F_{11}^1(k)} \qquad (2.2.5)$$

where $F_{11}^1(k_1)$ is the one dimensional spectrum, results like those shown in Figures 2-1 and 2-2 were obtained using Pao's spectrum for the turbulence. As for the hotwire, it is clear that disturbances smaller than the largest dimension of the volume cannot be measured.

There are a number of extensions and refinements which could be carried out. In particular: alternate formulations for the effective measured velocity could be constructed and their consequences explored, and the effect of alternate volume shapes ($w(\underline{x})$ different from Gaussian) could be calculated. It appears unlikely that any additional fundamental knowledge would be gained from these.

2.3 The Problem of Random Phase Fluctuations (Doppler Ambiguity)

In reference I, the authors were able to show that if an effective displacement field $\underline{x}_o$, was defined by

$$\underline{u}_o = \frac{d\underline{x}_o}{dt} \tag{2.3.1}$$

then the expression for the Doppler current (eqn. 2.1.1) could be reduced to

$$i(t) = (F^2+G^2)^{1/2} \cos (\underline{K}\cdot\underline{x}_o - \phi) \tag{2.3.2}$$

where

$$\tan \phi = \frac{G}{F} \tag{2.3.3}$$

Note that F, G, and ϕ are all time dependent and in general random quantities.

Most importantly, by assuming that the average number of particles in the volume was large ($\bar{N}>10$) and that relative displacements due to the turbulence were governed by Gaussian probability distributions, it was possible to show that the fluctuations of $\underline{x}_o$ (and hence $\underline{u}_o$) and those of F, G, and ϕ were statistically independent. This fact and the additional fact that F and G could be shown to be Gaussian random variables allowed immediate application of the large body of research on FM-noise which had developed over the past forty years.

It is not the purpose of this article to review all of the consequences of this on the design of continuous LDA processors, but rather to concentrate on those aspects which bear directly on the interpretation of measurements of turbulent velocities. For a more complete treatment the reader is referred to reference I and the papers by Duranni and Greated (1973), and George (1976)*.

The ideal signal processor would remove the amplitude information from equation (2.3.2) and yield an output proportional to the derivative of the total phase. Thus the "velocity-like" output of the detector, say $u_d(t)$,

* hereafter referred as reference II.

would be given by

$$u_d(t) = u_o(t) - K^{-1}\,\dot{\phi}(t) \tag{2.3.4}$$

Since the fluctuations u_o and $\dot{\phi}$ have been shown to be statistically independent, the statistical quantities of this output signal most often of interest have the following properties:

(i) The autocorrelations of u_o and $\dot{\phi}$ are additive

$$\overline{u_d(t)\,u_d(t')} = \overline{u_o(t)\,u_o(t')} + K^{-2}\,\overline{\dot{\phi}(t)\,\dot{\phi}(t')} \tag{2.3.5}$$

(ii) The spectra of u_o and $\dot{\phi}$ are additive

$$S_{u_d}(f) = S_{u_o}(f) + K^{-2} S_{\dot{\phi}}(f) \tag{2.3.6}$$

(iii) The mean square values of u_o and $\dot{\phi}$ are additive

$$\overline{u_d^2} = \overline{u_o^2} + K^{-2}\overline{\dot{\phi}^2} \tag{2.3.7}$$

(iv) The probability densities of u_o and $\dot{\phi}$ are convolved.

$$p_{u_d}(u) = \int_{\infty}^{\infty} p_{u_o}(x-u)\; p_{\dot{\phi}/K}(x)\,dx \tag{2.3.8}$$

Clearly it is not enough to be able to relate the volume-averaged velocity to the turbulence (section 2.2), but we must also have complete knowledge of $\dot{\phi}$ if we are to interpret the measurements. An unfortunate fact is that the spectral bands of u_o and $\dot{\phi}$ always overlap so that a simple removal of the phase fluctuations by filtering is not possible. In fact, there appears to be no way to avoid this contamination although there are several ways in which its effects can be minimized. These will be mentioned later.

2.4 The Statistics of the Phase Fluctuations

The reality of the phase fluctuations and their effect on attempts to measure turbulence from continuous signal processors is readily apparent from Figure (2-3) taken from Lading and Edwards (1976). The top trace represents the turbulent input signal to an LDA signal simulator while the bottom three traces represent the outputs of various continuous LDA processors. If there

were no random phase fluctuations in the signal, all four traces should be identical. Instead the bottom traces are similar and are distinctly different from the turbulence signal at the top. The high frequency contributions of the random phase fluctuations are readily apparent; more subtle, but still present, are the lower frequency contributions which overlap the frequency band of the turbulent fluctuations.

The statistics of the random phase fluctuations can be shown to be entirely determined by one parameter, $\Delta\omega$, called the Doppler ambiguity bandwidth (or broadening). $(\Delta\omega)^{-1}$ is, in fact, related to the time the envelope of the Doppler current remains correlated with itself and can be determined from the following

$$\frac{\overline{F(t)\,F(t')}}{\overline{F^2}} = \frac{\overline{G(t)\,G(t')}}{\overline{G^2}} = \exp\{-(\Delta\omega\,\tau)^2/2\} \qquad (2.4.1)$$

The rate at which the envelope becomes uncorrelated can be influenced by numerous effects. Of primary importance for turbulence measurement are: the loss of correlation because of the change in population of the scatterers, the loss in correlation due to the fact that mean gradients in the volume cause particles to beat against each other, and the same effect due to fluctuating gradients in the volume. These are referred to respectively as: transit time broadening, $\Delta\omega_L$; gradient broadening, $\Delta\omega_G$; and turbulence broadening, $\Delta\omega_T$. It can be shown that

$$(\Delta\omega)^2 = (\Delta\omega_L)^2 + (\Delta\omega_G)^2 + (\Delta\omega_T)^2 \qquad (2.4.2)$$

Each component can be calculated separately and the appropriate equations are shown in Table I. For details the reader is referred to reference I and Berman and Dunning (1973).

An example of the relative importance of these three effects can be found in the measurements of Berman and Dunning (1973) in a turbulent pipe flow. Near the center of the pipe where the mean gradient was small the

transit time and turbulence broadening terms were about equal and dominant. Near the wall, however, where both turbulence intensity and mean gradient were larger, the mean gradient and turbulence broadening dominated while the transit time broadening was negligible.

It is appropriate to note that there seems to have often been confusion regarding the turbulent broadening part, $\Delta\omega_T$. This broadening is quite independent of effect of the fluctuations in the effective velocity u_o which contribute directly to a broadening of the Doppler current spectrum (for further information see reference II).

Once $\Delta\omega$ is known, the above-mentioned statistical measures of $\dot{\phi}$ can readily be calculated from the relationships summarized in Table II (from Ref. II). These are plotted in Figures (2-4), (2-5) and (2-6). It is easy to show that $\overline{\dot{\phi}^2} = \infty$. This of course assumes that our ideal detector has an unlimited frequency response.

2.5 Implications of Phase Fluctuations on Turbulence Measurement

A number of implications of these results on attempts to measure turbulence are obvious. First, low turbulence intensity measurements are not something the continuous LDA does well. Second, measurements of autocorrelations at small time delays and spectra at high frequencies will be difficult or impossible. Third, the accuracy of probability density determination will be entirely dependent on whether $u' >> K^{-1}\Delta\omega$.

Figure (2-7) shows an attempt to measure an autocorrelation in a grid turbulence. The finite value of the correlation at zero-time delay reflects the finite bandwidth of the processor. Figure (2-8) shows a similar attempt to measure a velocity spectrum in a turbulent pipe flow. In this case, the high level of the turbulence spectrum relative to that of the phase fluctuations indicates that a reasonably accurate estimate of $\overline{u_o'^2}$ could be made if a filter were placed near the frequency at which the spectra are equal (shown by arrow).

A similar spectrum measured in a grid turbulence is shown in Figure (2-9). Filtering in this case would be less satisfactory.

It should be clear from the examples chosen that single point statistical measures can be taken with an LDA. It should also be clear that great care must be taken in interpreting the results. Moreover, significant benefits are to be gained if the ambiguity noise can be minimized. Means for doing this are discussed in the next section.

2.6 Minimizing and Eliminating the Effects of Phase Fluctuations on Turbulence Measurement

For any given flow situation there exists an optimal scattering volume size which minimizes the value of $\Delta\omega$ and hence the spectral level of the phase fluctuations. This is readily evident from equations (2.4.2) and Table I. For more detail and examples see George (1972), Berman and Dunning (1973) and reference I. The last of these also considered the trade-off between spatial resolution and minimizing the spectral height of the phase fluctuations; in almost all cases the phase fluctuations are responsible for the limiting conditions on spectral measurements.

A more imaginative approach to minimizing the effects of phase fluctuations is simply to try and eliminate some of them. Wilmshurst and Rizzo (1974), noting that the maximum phase spikes correspond to the minimum of the Doppler envelope, used a tracker error signal weighted with envelope amplitude, thereby eliminating a significant contribution to $\overline{\dot{\phi}^2}$. In fact, any real tracker discriminates against these large phase fluctuations by tracking the Doppler signal only when the envelope is above a given threshold. If the portion of the signal removed by this procedure is small compared to the length of the envelope (which is, in turn, usually much smaller than any flow time of interest), a significant reduction in $\overline{\dot{\phi}^2}$ appears to be possible. Unfortunately the implications of this on the phase fluctuation spectrum are not clear; that is, it is not clear whether the level of the phase fluctuation spectrum is reduced (the desired result) or whether only the high frequency

part of the spectrum is removed.* If only the latter, then the benefits are minimal.

George (1974) following a suggestion of Rowe showed that a sequence of low-pass filters could be used to make accurate turbulence intensity measurements of the spectrum of the zero-crossings, even when the contribution of the phase fluctuations was large. This technique has been successfully applied by numerous investigators to make reliable intensity measurements.

It is easy to show that the correlation of phase fluctuations between non-overlapping scattering volumes is zero, (references I & II). This implies that the continuous LDA can be successfully used for ambiguity-free, non-intrusive cross-correlation measurements. Examples of such use are Morton and Clarke (1971) and Reed (1978). Van Maanen et al (1976),following a suggestion of George (1971 and reference I),built a special optical system for correlating signals from two volumes within the smallest turbulence scale, thereby obtaining the ambiguity-free, single point turbulence spectrum.

In summary, it is possible to minimize the spectral level of the phase fluctuations in all situations by choosing the appropriate scattering volume. Moreover, even these phase fluctuations can often be dealt with directly by filtering or subtraction since their spectral level is known exactly once $\Delta\omega$ is known. Finally the continuous LDA is at its very best in measuring cross-correlations since it is both ambiguity free and non-intrusive (thus eliminating the familiar problem of the wake of the leading probe).

* It appears to be straightforward to extend Rice's calculations to include the spectrum of the level crossings. To the best of our knowledge this has not been done.

2.7 Dropout

No real tracker can track the fluctuating phase of the Doppler signal exactly. Momentarily or permanently the lock between tracker oscillator and signal may be broken and the tracker encounters a so-called drop-out. In modern trackers the tracking performance is monitored by a drop-out detector, which indicates the presence of a drop-out, when the correlation between the signal and the tracker oscillator falls below a preset level. Under normal operating conditions drop-out is associated with signal amplitude fluctuations caused by phase cancellations between many particles in the measuring volume rather than with the absence of particles in the volume. Since these amplitude fluctuations occur with time scales of the order of the particle transit time through the measuring volume, drop-out periods are normally short compared to the time scales of the flow. A typical drop-out case is illustrated in Figure 2-10, which shows at the bottom the Doppler signal, next the control voltage to the tracker oscillator and at the top the tracker output including drop-out periods, where the signal during drop-out has been replaced by the last measured value. As discussed earlier, drop-out can be beneficial if it discriminates against the largest phase fluctuations.

There are three ways of handling the signal during drop-out:

1. Setting the output equal to zero during drop-out,
2. setting the output equal to the mean during drop-out, and
3. holding the signal at its last value during drop-out.

In the following each of these alternatives are analyzed.

We first assume that the occurrence of drop-out and reacquisition of signal are statistically independent of the velocity, and that the fractional drop-out time is small and independent of velocity. This is a good approximation in the case of a many-particle continuous signal. The probability

that the Doppler signal amplitude R is below a given value, R_1 say, is given by (reference II):

$$P[r<R_1] = 1 - \exp\left[-\frac{R_1^2}{2\overline{i^2}}\right], \qquad (2.7.1)$$

where $\overline{i^2}$ is the mean-square Doppler signal. If the drop-out threshold is given, the fraction of time the tracker is in drop-out condition can readily be computed.

Lumley, Buchhave and George (1978) suppose that the drop-out times are independently distributed with a probability of a drop-out in any interval dt of μdt. They further suppose that the drop-out process is a Markov chain so that μdt is the transition probability from "in" to "out". The transitions to the tracking condition are also independently distributed with a transition probability from "out" to "in" in the interval dt of νdt. Thus the expected "in-time" is $1/\mu$, and the expected "out-time" is $1/\nu$. (The latter corresponds to the result computed from the amplitude probability distribution above). The probability of being "in" at any instant is $(1+\mu/\nu)^{-1}$, while the probability of being "out" is $(1+\nu/\mu)^{-1}$. For all cases of interest $\nu/\mu<<1$, which is to say that the tracker is "in" most of the time.

To analyze the tracker output an indicator function I(t) was defined as +1 when the tracker is "in" and 0 when the tracker is "out". The expected value of I is clearly $\overline{I} = (1+\mu/\nu)^{-1}$. The tracker output signal can thus be represented as

$$\tilde{f}(t) = f(t) \cdot I(t), \qquad (2.7.2)$$

where f(t) is the output without drop-out (the tracker response to the instantaneous velocity).

Case 1: Output equal to zero during drop-out.

We consider the statistics of $\tilde{f}$ given by equation (2.7.2). It is

straightforward to show that the mean is given by

$$\bar{\tilde{f}} = \bar{f} \cdot \bar{I} = \bar{f} \cdot \left(\frac{\nu}{\nu+\mu}\right) \tag{2.7.3}$$

while the mean-square fluctuation is given by

$$\overline{\tilde{f}'^2} = \overline{f'^2} \cdot \overline{I^2} + \left[\bar{f}^2 + \overline{f'^2}\right] \overline{I'^2} \tag{2.7.4}$$

I(t) can be shown to have a mean-square value given by

$$\overline{I'^2} = \bar{I}(1-\bar{I}) = \frac{\mu\nu}{(\mu+\nu)^2} \simeq \frac{\mu}{\nu} \tag{2.7.5}$$

and an autocovariance function given by

$$R_I = \frac{\mu\nu}{(\mu+\nu)^2} e^{-(\mu+\nu)|\tau|} \simeq \frac{\mu}{\nu} e^{-\nu|\tau|} \tag{2.7.6}$$

The analysis leads to the following expressions for the autocorrelation and spectrum of $\tilde{f}$

$$R_{\tilde{f}} = \bar{I}^2 R_f + \bar{f}^2 R_I - R_f R_I \tag{2.7.7}$$

and

$$S_{\tilde{f}} \simeq S_f + \frac{\mu}{\pi\nu^2}\left(\bar{f}^2 + \overline{f'^2}\right)\left(\frac{1}{1+(\omega/\nu)^2}\right) \tag{2.7.8}$$

To get this particular form for the spectrum we have assumed that the periods between drop-outs $1/\mu$ are short compared to the integral scale T. The effect of the drop-out is to add a spike to the autocovariance and a low-passed white noise to the spectrum. The amount of noise is determined by the mean square of the total signal (i.e. mean plus fluctuating component). If the periods between drop-outs are long compared to the integral scale, R_f will dominate in the last term of equation (2.7.7) and the effect of the drop-out is merely a slightly reduced record length, but no significant addition of noise.

Case 2: Output set equal to mean during drop-out.

We can represent the tracker output as follows:

$$\tilde{f}(t) = f(t)\, I(t) + \bar{f} \cdot [1-I(t)] \tag{2.7.9}$$

It is easy to show that the mean is preserved in this case, i.e. $\overline{\tilde{f}} = \overline{f}$ The mean-square fluctuation, the autocorrelation, and the spectrum are given by equation (2.7.4), (2.7.7), and (2.7.8) respectively with $\overline{f}$ set equal to zero. Thus the noise level introduced by the drop-out on these measurements is considerably reduced since the spectral height of the noise, for example, is now determined only by the drop-out and the mean-square fluctuating signal.

Case 3: Output holds last value

This method is common practice in commercial trackers. The output signal can be represented by:

$$\tilde{f}(t) = f(t)I(t) + \hat{f}(t)\,[1-I(t)] \qquad (2.7.10)$$

where

$$\hat{f}(t) = f(t_k) \text{ for } t_k \leq t < t_{k+1} \qquad (2.7.11)$$

and t_k (k=1,2,...) are the drop-out times.

It is easy to show that in this case the mean and all higher moments of $\tilde{f}$ are identical to those of f. Thus, not only are the mean velocity and the turbulence intensity accurately reproduced, but also the entire probability density. Some noise is still present in the spectrum, but under normal conditions the spectral noise power will be considerably lower than in the previous case. The autocovariance can be computed from from equation (2.7.10) as

$$R_{\tilde{f}} = \overline{I}^2 R_f + (R_f + R_{\hat{f}} - 2R_{f\hat{f}})\, R_I + 2\overline{I}(1-\overline{I})R_{f\hat{f}} \qquad (2.7.12)$$

Assuming again $T \gg 1/\nu$ and $1/\mu$ we see that the autocovariance is dominated by the first term, which is the desired autocovariance of the signal, and the second term, which is a spike at the origin of duration $\simeq 1/\mu$ and a magnitude determined by the difference $R_f + R_{\hat{f}} - 2R_{f\hat{f}}$, which for $1/\mu \ll T$ is small compared to $\overline{f'^2}$. Thus the noise term in the spectrum will be significantly reduced relative to the previous case:

$$S_{\tilde{f}} \simeq S_f + \frac{\mu}{\pi\nu^2}\,\overline{(\Delta f)^2}\left[\frac{1}{1+(\omega/\nu)^2}\right] \qquad (2.7.13)$$

where $\overline{(\Delta f)^2}$ represents the difference $2(\overline{f'^2} - R_{ff}\hat{}(o)) << \overline{f'^2}$

Considering the other extreme, $1/\nu >> T$, we must have $R_{ff}\hat{} \simeq 0$, since f(t) will now most likely be uncorrelated with its value at the previous drop-out. At the same time $R_f\hat{} \simeq \overline{f'^2}\, R_I$ so that $R_f\hat{}R_I \simeq \overline{f'^2}\, R_I^2$ and also $R_f R_I \simeq (\overline{I}-\overline{I}^2)R_f$. Thus the autocovariance reduces to

$$R_{\tilde{f}} \simeq \overline{I}\, R_f + (1-\overline{I})\overline{f'^2}\, R_I^2 \qquad (2.7.14)$$

For long drop-out times method 3 is more noisy than setting the output to zero during drop-out. However, $1/\nu << T$ is not the usual mode of operation for the tracker.

In summary, drop-out can affect all statistical properties of the tracker output. The magnitude of this effect depends on the manner in which the tracker compensates for this drop-out. In the most usual mode of operation of the tracker, where drop-outs are short compared to the flow integral scale, drop-out is best handled by maintaining the last measured output until the tracker has again acquired lock. This method preserves all moments of the velocity distribution, and adds the least amount of noise to the spectrum. Higher order approximations during drop-out can be envisioned, e.g. linear extrapolation from the last measured value. Such methods might further reduce noise in tracker output, but has to the best of our knowledge not been tried in practice. If drop-out periods long compared to the integral scale occur, it might be best to set the output equal to a running average of previously measured values.

3. BURST SIGNAL PROCESSING

3.1 Signal Processor Function

The operation of the burst signal processor (single particle measurement or individual realization)differs radically from that of the quasi-continuous type signal processor. Whereas the latter in its normal mode of operation presents a continuous output, possibly interspersed with periods of drop-out, the former detects the velocity of individual particles and in most cases bases the velocity output on a measurement of the time of flight across the measuring volume (or across a fixed number of interference fringes in the measuring volume). Knowing the fringe spacing, the timing information is equivalent to a velocity sample. The velocity sample is computed and presented at the output after the particle traversal, usually as a digital word, and thus does not represent a real-time analog output. The function of the processor is inherently a digital, random sampling of the velocity at a point in time determined by the particle arrival. In some processors the real-time clock is also used to provide the time increment between samples allowing, as we shall discuss later in this section, the formation of the velocity autocovariance and spectrum from the randomly sampled data. If the seeding concentration is sufficiently high, a continuous analog output can be obtained through a D/A converter, but in most cases of interest, the data rate would be below that required to resolve small scale turbulent fluctuations in a real-time mode. Thus, the main problem in burst detection LDA signal processing is the extraction of statistical quantities from the randomly sampled data accumulated by the processor.

The best optical configuration for single particle detection is the dual-beam, fringe mode system which optimizes the collection of light from single scattering particles. In the absence of particles in the measuring volume, the detector output is shot noise due to ambient light and laser light reaching

the detector from optical surfaces and windows. The photocurrent is thus a band limited shot noise signal superimposed on randomly arriving Doppler bursts. Mayo (1975) suggests a triply stochastic model for the burst signal:

$$i(t) = \sum_{i=-\infty}^{\infty} e\, g_i \cdot h(t-t_i) \qquad (3.1.1)$$

where e, g_i and h(t) are respectively electronic charge, the random charge gain of the detector preamplifier and the impulse response of the detector/preamp/filter system. t_i is the random time for the occurrence of the i^{th} photoelectron. This process is a modulated Poisson process (known as a Mandel-process from photon counting theory), where the modulating function is the statistical mean photoelectron rate $\lambda(t)$, which in turn is related to the classical optical power at the detector p(t) by:

$$\lambda(t) = \frac{\eta p(t)}{h\nu} \qquad (3.1.2)$$

where η is detector efficiency and $h\nu$ the photon energy. p(t) reflects the superposition of the background photoelectron arrival rate λ_b and the randomly arriving bursts:

$$p(t) = \frac{h\nu}{\lambda}\left[\lambda_b + \sum_{j=-\infty}^{\infty} I_j\, f(t-\tau_j, \underline{u}_j, \underline{r}_j)\right], \qquad (3.1.3)$$

where I_j is a random peak amplitude parameter determined by particle size and scattering function and $f(t,\underline{u},\underline{r})$ is a normalized optical system response function. τ_j thus marks the peak of a burst. As indicated f, which specifies the burst shape, is in general a function of particle velocity $\underline{u}_j$ and particle trajectory parameter $\underline{r}_j$.

The triply stochastic nature of the photodetector signal is evident from this model. The occurrence of the photoelectron at t_i is a Poisson process modulated by the instantaneous classical optical power p(t). p(t) is in turn a stochastic

process determined by the particle arrival times τ_j, which are again distributed as a modulated Poisson process. The function modulating the burst arrival times is determined by the velocity time function $\underline{u}(t)$ and possibly other effects correlated with the velocity. The velocity may itself be a stochastic function, e.g. Gaussian random turbulence. Mayo (1977)provides a FORTRAN program for the simulation of a burst signal, which allows evaluation of signal processor performance from assumed models of the statistical processes entering the signal synthesis.

With sufficiently high laser power, the background current may be neglected and the signal-to-noise ratio of the detector current (defined as the signal variance relative to the square of the signal mean at the peak of the burst) high enough to allow the burst wave form to be set equal to the classical optical pulse. For the case of two Gaussian laser beams of equal power intersecting in a common focal volume as illustrated in Figure 1-2, we retrieve the well-known Gaussian burst in the limit of infinite signal-to-noise ratio:

$$i_j(t) = I_j w(\underline{x}_j(t)) \, [1 + \cos(\omega_D t)], \qquad (3.1.4)$$

where $\underline{x}_j$ is the particle trajectory, ω_D the Doppler frequency and $w(\underline{x})$ is given by equation (2.2.4).

3.2 The Velocity Measured by Burst Processors

Representation

Unlike the case with the continuous LDA where we were able to only postulate the form of the measured velocity and then show that this form was reasonable, for the burst processor we can write directly the velocity signal since there are assumed to be only single particles present. Thus the velocity measured by the ideal burst processor is exactly the velocity of the particle producing the burst. The only question is whether the randomly arriving samples are capable of reproducing the statistics of the

desired Eulerian velocity field. We shall see that the answer to this question is in the affirmative if the burst signal is analyzed for the period of time the particle is in the volume.

To examine this further we write for the measured velocity

$$u_0(t) = \int w[\underline{x}(\underline{a},t)]\, u(\underline{a},t)\, g(\underline{a})\, d^3\underline{a} \tag{3.2.1}$$

in the same form as that assumed for the continuous case.* In effect, this reproduces the instantaneous velocity of the scattering particle only while it is in the scattering volume. A typical $u_0(t)$ is shown in Figure (3-1). Assuming incompressibility and mapping from the Lagrangian to the Eulerian frame this can be written

$$u_0(t) = \int w(\underline{x})\, u[\underline{x}(\underline{a},t)]\, g_1(\underline{x},t)\, d^3\underline{x} \tag{3.2.2}$$

where

$$\underline{x} = \underline{a} + \int_0^t \underline{u}(\underline{a},t_1)dt_1 \tag{3.2.3}$$

and

$$g(\underline{a}) \to g_1(\underline{x},t). \tag{3.2.4}$$

The statistics of $g_1(\underline{x},t)$ for statistically uniform seeding to 2nd order can be shown to be given by (George, Buchhave, and Lumley, 1978).**

$$\overline{g_1(\underline{x},t)} = \mu \tag{3.2.5}$$

$$\overline{g_1(\underline{x},t)\, g_1(\underline{x}',t')} = \mu p(\underline{x},t \mid \underline{x}',t') + \mu^2$$

where $p(\underline{x},t|\underline{x}',t')$ is the probability that the particle at $\underline{x}$ at time t has moved to $\underline{x}'$ at time t' and μ is the expected number of particles per unit volume. An excellent approximation to $p(\underline{x},t|\underline{x}',t')$ for all practical purposes is:

$$p(\underline{x},t|\underline{x}',t') \to \delta(\underline{x}'-\underline{x}-\underline{U}\tau) + \mu^2 \tag{3.2.6}$$

* The average over the number of particles in the volume is no longer necessary since, by hypothesis, there is never more than one.

** References I and II ignored the time dependence of the g function. The differences, with one exception, are inconsequential.

Mean Values

Once the above problem for the statistics of $q_1(\underline{x},t)$ is uncoupled from the statistics of the velocity field, then it is straightforward to show that the average of u_o is given by

$$\overline{u_o(t)} = \mu \int \overline{u(\underline{x},t)} \quad w(\underline{x}) d^3\underline{x} \tag{3.2.7}$$

To understand the implications of this consider the simple case where $\overline{u(\underline{x},t)}$ is independent of $\underline{x},t$ and $w(\underline{x},t) = 1$ within the volume and zero outside. (Note that these correspond to a uniform mean velocity and an on-off scattering volume; the on-off volume is an excellent approximation to the volume seen by a burst processor if we ignore the angle effects discussed later). Assuming this, we have

$$\overline{u_o(t)} = \mu V \, \overline{u(x,t)} \tag{3.2.8}$$

Thus the measured mean velocity is directly proportional to the desired Eulerian mean. It should not be inferred from this that one needs merely average realizations to achieve reasonable averages. Equation (3.2.8) assumes that the velocity has been measured during all of the time the particle is in the volume and the factor μV accounts for the portion of time that it is not.

To see this, assume that we are determining the mean values by time-averaging.

$$\overline{u_o(t)} \simeq \frac{1}{T} \int_o^T u_o(t) dt \tag{3.2.9}$$

where it is assumed that T is sufficiently long. Eqn. (3.2.8) implies that

$$\overline{u_o(t)} \simeq \frac{1}{T} \int_o^T u_o(t) dt = \mu V \frac{1}{T} \int_o^T u(\underline{x},t) dt \simeq \mu V \, \overline{u(\underline{x},t)} \tag{3.2.10}$$

where $\overline{u}(\underline{x},t)$ is the information we desire. Then it follows that

$$\overline{u(x,t)} \simeq \frac{1}{\mu V T} \int_o^T u_o(t) dt \tag{3.2.11}$$

But μVT is exactly the fraction of time that the signal $u_o(t)$ is non-zero. Thus, the correct mean is given by averaging only during those periods where there is a signal.

Most real processors measure the average velocity during the burst; this implies that the velocity must be approximately constant during its traversal of the volume. Moreover, since there is only a single realization during each particle passage, then the realization must be weighted by the time the particle would contribute to the integral; that is, the residence (or transit) time. This is easily seen by approximating $u_o(t)$ as constant while there is a signal and writing the integral as a sum:

$$\overline{u(\underline{x},t)} = \frac{1}{\mu VT}\int_0^T u_o(t)dt \approx \frac{\sum_i u_o(t_i)\Delta t_i}{\sum_i \Delta t_i} \qquad (3.2.12)$$

where $u_o(t_i)$ represents the i^{th} realization and Δt_i the residence time of that particle. Note that the direction of the particle and its velocity are irrelevant; only its x-component and residence time matter.*

The idea of transit time weighting of the realizations and the preceding proof were first presented by George in 1975 (reference I). Hosel and Rodi (1977) later presented a less rigorous derivation based on mean transit times and successfully applied it to measurements of mean velocity in a jet. Some commercial burst processors now provide the residence time information necessary for using equation (3.2.12) and those derived below.

Turbulence Intensities

Now we examine the second order statistics of the effective velocity. We square and average equation (3.2.2) and apply the results of equation (3.2.5) to obtain

$$\overline{u_o(t)u_o(t')} = \mu\iint w(\underline{x})\, w(\underline{x}')\, \overline{u(\underline{x},t)u(\underline{x}',t')}\, p(\underline{x},t|\underline{x}',t')\, d^3\underline{x}\, d^3\underline{x}'$$
$$+ \mu^2\iint w(\underline{x})\, w(\underline{x}')\, \overline{u(\underline{x},t)\, u(\underline{x}',t')}\, d^3\underline{x}\, d^3\underline{x}' \qquad (3.2.13)$$

* The residence weighting may be viewed as a correction, which creates an effective sample rate independent of velocity; referring to Figure (3-2), the actual sample rate is seen to be $R = \mu A|\underline{u}|$. The effective sample rate of residence time weighted samples may be written:

$R_C = \overline{\Delta t} \cdot \mu \cdot A \cdot |\underline{u}| = \frac{\overline{\ell}}{\underline{u}} \cdot \mu A|\underline{u}| = \mu \cdot V$, where V is the volume of the measuring volume, $\overline{\Delta t}$ is the mean residence time for particles with velocity $\underline{u}$ and $\overline{\ell}$ is the corresponding average trajectory length through the measuring volume. The resultant rate is just the average number of particles in the volume, independent of $|\underline{u}|$.

We first consider the case $t = t'$ for which $p(\underline{x},t|\underline{x}',t') = \delta(\underline{x}-\underline{x}')$ This case is of particular interest since it, in fact, corresponds to the mean square velocity. From equation (3.2.13) we obtain:

$$\overline{U_o}^2 + \overline{u_o'^2} = \mu\left[\overline{\int w^2(\underline{x})\, U^2(\underline{x})\, d^3\underline{x}} + \int w^3(\underline{x})\, \overline{u'^2(\underline{x})}\, d^3\underline{x}\right]$$

$$+ [\text{terms of order } (\mu V)^2] \qquad (3.2.14)$$

The second term is negligible compared to the first and is not of interest here since we are interested only in individual realization anemometry where the particle concentration is low. (Note that the reverse was true for the continuous LDA where the first term was neglected with respect to the second).

It is clear that we can readily identify the mean square fluctuation we desire in equation (3.2.14) if $U(\underline{x})$ = constant. Again assuming $w(\underline{x}) = 1$ within the volume and zero outside, and assuming $\overline{u'^2}$ to be constant over the volume, we obtain

$$\overline{u_o'^2} = \mu V\, \overline{u'^2} \qquad (3.2.15)$$

Analysis of this in terms of time integrals leads to the same conclusion as before: The residence time weighted average provides the correct mean square fluctuating velocity (reference II). Thus

$$\overline{u'^2} = \frac{\sum_i [u(t_i)-U]^2 \Delta t_i}{\sum_i \Delta t_i} \qquad (3.2.16)$$

where U is computed from equations (3.2.12)

It is tedious but straightforward to interpret equations (3.2.7) and (3.2.1 for non-ideal scattering volumes and non-uniform velocities. The only differenc is that now volume-averaged information is obtained. The effect on the statistics of this volume averaging is identical to that in the continuous case mentioned earlier. Note that the presence of a mean gradient will contribute an apparent turbulence intensity even when no turbulence is present because of the contribution of the first term in equation (3.2.14). A particular problem

associated with directional effects of real finite volume processors is discussed in Section (3.3).

Correlations and Spectra

We now examine the possibility of measuring autocorrelations and spectra with burst processors. The correlation of the measured velocity is readily computed to be

$$\overline{u_o(t)\, u_o(t')} = \iint \overline{u(\underline{x},t)\, u(\underline{x}',t')}\, w(\underline{x})\, w(\underline{x}')\, g_1(\underline{x},t) g_1(\underline{x}',t') \cdot d^3\underline{x}\, d^3\underline{x}' \tag{3.2.17}$$

Applying equations (3.2.5) and (3.2.6) we have

$$\overline{u_o(t)\, u_o(t+\tau)} = \mu \underbrace{\iint \overline{u(\underline{x},t)\, u(\underline{x}',t')}\, w(\underline{x})\, w(\underline{x}')\, \delta(\underline{x}'-\underline{x}-\underline{U}\tau)\, d^3\underline{x}\, d^3\underline{x}'}_{I(\tau)}$$

$$+ \mu^2 \underbrace{\iint \overline{u(\underline{x},t)\, u(\underline{x}',t')}\, w(\underline{x})\, w(\underline{x}')\, d^3\underline{x}\, d^3\underline{x}'}_{II\ (\tau)} \tag{3.2.18}$$

In the succeeding analysis we shall show that the first term contributes only for very short time lags ($\tau < d/U$) whereas the second produces the volume-averaged correlation (or spectrum) in the same manner as for the continuous signal and is therefore the desired result.

We consider the first term only for now. Carrying out the integration over the delta function we obtain

$$I(\tau) = \mu \int \overline{u(\underline{x},t)\, u(\underline{x}+\underline{U}\tau, t+\tau)}\, w(\underline{x})\, w(\underline{x}+\underline{U}\tau) d^3\underline{x} \tag{3.2.19}$$

If the turbulence is assumed frozen, the space-time correlation of the fluctuating component reduces to the turbulence intensity, i.e.

$$\overline{u'(\underline{x},t)\, u'(\underline{x}+\underline{U}\tau, t+\tau)} = \overline{u'^2(\underline{x})}$$

and we are left with

$$I(\tau) = \mu \int \left| \overline{\underline{U}(\underline{x})\, U(\underline{x}+\underline{U}(\underline{x})\tau) + \overline{u'^2(\underline{x})}} \right| w(\underline{x})\, w(\underline{x}+\underline{U}(\underline{x})\tau) d^3\underline{x} \tag{3.2.20}$$

Thus the contribution of the first term to the autocorrelation is simply a contribution determined by the volume and the mean transit time of the particles.

For the case where the mean velocity is uniform and turbulence homogeneous this reduces to

$$I(\tau) = \mu V\left[\overline{U^2} + \overline{u'^2}\right] \rho_I(\tau) \tag{3.2.22}$$

where

$$V\rho_I(\tau) = \int w(\underline{x})\, w(\underline{x} + \underline{U}\tau) d^3\underline{x} \tag{3.2.23}$$

For the case where $w(\underline{x}) = 1$ inside and zero outside the volume, this is simply a spike at the origin of unit height whose width is proportional to the mean transit time of the particles through the volume ($\sim d/U$). Note that equation (3.2.22) reduces to the result obtained in the previous section for $\tau = o$ as it should.

Since this first term $I(\tau)$ contains no information of interest except at $\tau=o$, it can be considered noise which it is desirable to eliminate. Fortunately, this is easily done with the autocorrelation since time lags of the order of a particle transit time are seldom of interest in turbulence. This is always the case if the streamwise extent of the scattering volume is smaller than the Kolomogorov microscale. A less restrictive condition might be $d << \lambda_u$ where λ_u is the spatial Taylor microscale for the u-component of velocity and characterizes the small τ behavior of the autocorrelation (since $\lambda_\tau = \lambda_u/U$).

It is straightforward to show that this unwanted information contributes over the entire frequency range of the spectrum to $\omega \sim \tau_o^{-1}$ with height $S_I(\omega) \sim \mu V\,[U^2 + \overline{u'^2}]\tau_o$ and rolls off as ω^{-2} thereafter where τ_o is the transit time. Note that the magnitude of this term can be considerably increased if significant velocity gradients are present across the volume.

It will be seen below that in most burst-processing applications this completely swamps the desired spectrum which is proportional to $(\mu V)^2$. (Recall that μV is expected number of particles in the volume, and is generally much less than unity). Fortunately, since the correlation of this "transit time noise" is confined to near the origin, it can be eliminated in most applications by removing it from the correlation before transforming to obtain the

spectrum.

We consider now the second term and recognize it to be similar to the term we retained in the analysis of continuous signal processors (Chap. 2). Decomposing the velocity into mean and fluctuating parts yields

$$II(\tau) = \mu^2 \iint U(\underline{x})\, U(\underline{x}')\, w(\underline{x})\, w(\underline{x}')\, d^3\underline{x}\, d^3\underline{x}$$

$$+ \mu^2 \iint \overline{u'(\underline{x},t)\, u'(\underline{x}',t')}\, w(\underline{x})\, w(\underline{x}')\, d^3\underline{x}\, d^3\underline{x}' \qquad (3.2.24)$$

The first term is precisely the square of the volume-averaged mean velocity given in equation (3.2.7) and the second represents a volume-averaged space-time correlation. If we assume a uniform mean velocity and a frozen turbulence we can write, using the volume averaged spectrum of section 2.2

$$II(\tau) = U_o^2 + (\mu V)^2\, B_V(\tau) \qquad (3.2.25)$$

where

$$B_V(\tau) = \int e^{i\underline{k}\cdot\underline{U}\tau} F_m(\underline{k}) d^3\underline{k}$$

$$= \int \overline{u'(\underline{x},t)\, u'(\underline{x},t')}\, w(\underline{x})\, w(\underline{x}')\, d^3\underline{x}\, d^3\underline{x}' \qquad (3.2.26)$$

Clearly $B_V(\tau)$ is the desired information.

Combining $I(\tau)$ and $II(\tau)$ we have

$$\overline{(u_o(t)-U_o)(u_o(t')-U_o)} = (\mu V)\left|\overline{\underline{U}^2+\underline{u}'^2}\right| \rho_I(\tau) + (\mu V)^2\, B_V(\tau) \qquad (3.2.27)$$

Since $\mu V << 1$, the second term is substantially smaller. However, since the first term is zero for all $\tau > d/U$, the second term can still be obtained for all but the smallest time lags. This is not the case with the spectrum, however, which will be completely dominated by the first term.

It is easy to improve the situation by first computing the autocorrelation from the randomly arriving samples, then keeping only the part for which $\tau > d/U$. If the transit time is indeed less than any time lag of interest,

the remainder of the autocorrelation can be transformed to yield the spectrum. Since the value of the autocorrelation at $\tau = o$ has been obtained by the earlier analysis of $\overline{u'^2}$(equations 3.2.15) and 3.2.16), this value can be used to replace the missing information at the origin. Moreover, since we know that the autocorrelation is parabolic at the origin, the gap can be substantial (relative to λ) before we lose any information about the fluctuating velocity field. Thus the desired information about the autocorrelation is given by the second term as

$$\overline{u'(t)u'(t+\tau)} = (\mu V)^{-2} \frac{1}{T} \int u'_o(t)\, u'_o(t+\tau)\, dt \qquad (3.2.28)$$

where we have replaced ensemble averages by time averages.

In practice the elimination of the spike at the origin can be accomplished by simply not considering products of realizations with themselves, but only those products of realizations with other particles. It is important to note that the autocorrelation (or any cross correlation) cannot be computed simply by multiplying different realizations, grouping and averaging, as this introduces a bias (see §§ 3.3, 3.5).

The analysis above shows that if we consider the particle to contribute to the signal while it is in the volume, all of the desired statistical information can be obtained. As a consequence, the autocorrelation for a lag τ can be computed only when there is a particle in the volume at t and one at $t+\tau$. This is illustrated in Figure (3-3). The interpretation of this analysis leads to the following approximation to equation (3.2.28):

$$\overline{u'(t)\, u'(t+\tau)} \equiv \frac{\sum_{i,j} u'(t_i)\, u'(t_j)\, \Delta t_{ij}}{\sum_{i,j} \Delta t_{ij}} \qquad (3.2.29)$$

where $\tau = t_i - t_j$, $i<j$ and Δt_{ij} is the overlap time of the i^{th} realization and the j^{th} realization displaced by time τ. The denominator is essentially the

total overlap time corresponding to realizations of $u(t)\ u(t+\tau)$ since $(\mu V)^2 T \simeq \sum_{i,j} \Delta t_{ij}$. The overlap time is difficult to obtain in practice; an equivalent estimator for individual realizations is proposed in Section 3.5.

Similar considerations can be applied to single and joint probability densities, and to cross-correlations of different signals. Again the algorithm must be determined by the time the one or more signals actually contribute to the appropriate time integral expression. These are discussed in detail in Buchhave (1978) and George et al (1978).

3.3 Processing the Uncorrected Signal

Various methods of implementing residence time weighting have been suggested, but before discussing these and other correction techniques we shall briefly review the effects of processing the sampled data without applying any corrections. The fact that the particles cross through the measuring volume at a rate proportional to the instantaneous velocity (given uniform particle distribution) gives rise to bias errors when statistical quantities are formed by direct ensemble averaging of the accumulated sample values. However, the bias effect associated with the fluctuating velocity is only one of a number of possible biasing effects occurring in burst-type LDA processing. The sampling rate may also be correlated with velocity direction and with fluctuations in particle concentration resulting from density fluctuations, mixing of different fluids,or chemical reactions.

Assuming initially uniform scattering particle concentration and uniform density there are two main sources of bias associated with the velocity of the fluid through the measuring volume: correlation between sampling rate and velocity vector magnitude,and variation of the probability of a measurement with velocity direction (variation of measuring volume cross section). Referring to Figure (3-3), the rate at which particles cross the measuring

volume is given by $R = \mu A|\underline{u}|$ where A is the cross-sectional area of the measuring volume normal to the streamlines. We operate with the usual assumptions in burst detection that the velocity does not change appreciably during the time it takes a particle to cross the volume and that the probability of more than one particle in V at any time is negligible. Most signal processors, however, require a minimum number of zero crossings to execute a measurement. This fact has the effect of reducing the effective cross sectional area of the probe volume in a given direction to a value smaller than the geometrical cross section of the probe volume and results in "dead angles" in which no measurement is possible. Buchhave (1976) investigated the effect of the variation of cross-section with flow direction on bias in LDA-counter measurements and showed the effect to be significant and of the same order of magnitude as the velocity magnitude effect. Expressing the cross section in terms of the velocity components u, v, and w we may write

$$A(\underline{u}) = abc\,\frac{P}{u}\left(1 - \frac{a^2}{u^2}P^2Q^2\right) \tag{3.3.1}$$

where

$$P^2 = \frac{u^2}{a^2} + \frac{v^2}{b^2} + \frac{w^2}{c^2} \tag{3.2.2}$$

and a, b, and c are given by equation (1.1.1). $Q \equiv N_e/N_f$ is the ratio of N_e, the minimum number of zero crossings or fringe crossings required for a measurement, to N_f, the maximum number of fringe crossings available (corresponding to a particle trajectory along the x-axis). When $Q \to 0$, A approaches the geometrical cross section of the ellipsoidal probe volume, while increasing values of Q reduces A, increases the directional dependence and introduces dead angles. Figure (3-4) is a plot of A for particle trajectories parallel to the x,y-plane (normalized with respect to the geometrical cross section normal to the x-axis), versus ϕ, the angle between $\underline{u}$ and the x-axis. These curves are valid for a monidisperse particle distribution. Measured angular characteristics tend to show a less pronounced dead angle effect due to the presence of large particles.

The velocity bias effect on the formation of ensemble averages from LDA burst signal processors was first studied by McLaughlin and Tiederman (1973) for the limited case of Q = 0 and a spherical measuring volume. Using expressions (3.3.1) and (3.3.2) and assuming a data rate given by $R = \mu|\underline{u}|A$, Buchhave (1976) later repeated the analysis including the directional dependence of the cross section for various velocity distributions. Figure (3-5) shows the results for an assumed Gaussian velocity distribution superimposed on a constant mean velocity. The McLaughlin-Tiederman analysis corresponds to the curves for Q = 0. As is evident from the figure, direct mean and rms values from the accumulated data result in gross errors for turbulence intensities above $\sim$ 10%, and the errors increase as the angular dependence increases. The effect of bias is also visible in velocity histograms formed from the measured data. Figure (3-6)(McLaughlin and Tiederman (1973))illustrates the resulting skewness in the measured velocity distribution. The correlation between data rate and velocity also results in bias in steady flow when gradients are present within the measuring volume. Kreid (1974) predicted the errors introduced by steady gradients within the volume and found good agreement between measured and calculated bias errors in laminar pipe flow. Figure (3-7) shows the expected gradient bias errors according to these calculations.

3.4 Bias Correction

In introducing this section it is important to recall that in Section 3.2 it was shown that if time averages were formed by integrating only during the time measurement (i.e., only during particle residence times), no bias would exist. For example, the mean velocity can be approximated by the sum of products of trajectory-averaged velocity values and residence times in an unbiased manner by

$$U = \frac{\sum_i u_i \Delta t_i}{\sum_i \Delta t_i} \qquad (3.4.1)$$

u_i corresponds to the quantity measured by most burst type LDA signal processors. Thus complete velocity bias correction is achieved (or better, bias is avoided altogether) if in addition to the velocity output a measurement of the residence time is made available at the processor output to be used as a weighting factor in the computation of statistical quantities.

McLaughlin & Tiederman (1973) suggested a bias correction for one component measurements, which has since been used by a number of investigators. By weighting each sample by a weighting factor inversely proportional to the measured velocity component of the i^{th} sample, u_i, a correction of the computed statistical quantities results, which gives correct values in the case of one-dimensional flow fluctuations or steady flow, but overcompensates, when the velocity is fluctuating in two or three dimensions. Another limitation is that the one dimensional correction does not take into account any directional dependence of the measurement cross section. Using the weight $|u_i|^{-1}$ the expressions for the corrected mean and mean square fluctuating values become:

$$U = \frac{\sum_{i=1}^{N} |u_i|^{-1} u_i}{\sum_{i=1}^{N} |u_i|^{-1}} = \frac{N}{\sum_{i=1}^{N} |u_i|^{-1}} \tag{3.4.2}$$

and

$$\overline{u'^2} = \frac{\sum_{i=1}^{N} |u_i|^{-1} [u_i - U]^2}{\sum_{i=1}^{N} |u_i|^{-1}} \tag{3.4.3}$$

Figure (3-8) shows expected errors in mean and rms velocity measurements assuming a three-dimensional Gaussian velocity distribution and the application of the one-dimensional weighting factor. Again the curves for Q = 0 correspond to the analysis by McLaughlin and Tiederman, while other Q-values correspond to cases where the finite fringe number requirement introduces additional angular dependence. The one-dimensional correction reduces the bias errors, but beyond approximately 15% fluctuations relative to the mean the errors increase quite steeply. However, for a value of Q about 0.2 (corresponding to e.g. 8 zero-crossings out of 40) the directional dependence of the measurement cross section is seen to balance to some degree the over-compensation introduced by the one-dimensional bias correction.

Bias effects and the various correction methods are presently being studied by a number of investigators. It still has not been firmly established under which conditions the assumptions leading to the expressions for the data rate in Equations (3.4.2)and (3.4.3) are valid. Some investigators have reported a weaker correlation between data-rate and velocity than expected from these expressions (e.g. Smith and Meadows, 1974). Recent measurements by Karpuk and Tiederman (1976) and Quigley and Tiederman (1977) in the viscous sublayer in pipe flow show good agreement between mean and rms values computed from LDA single particle measurements corrected by one-dimensional weighting and hot-wire data. The measurements were made with an optical system specially designed to give a probe volume with small spatial dimensions in the direction of the mean velocity gradient. The authors note that the data rate did not seem to be correlated with direction, but did not indicate the ratio of the total number of fringes needed for the signal processing to the number available.

Recently Erdman and Gellert (1976) have studied the correlation between velocity and particle arrival rate and have shown very good correlation in an air flow modulated by an acoustic horn up to frequencies where particle lag influences the particle motion.

Although the one-dimensional correction is of interest because it is relatively simple to implement and gives good results in steady or one-dimensional flow, it seems more promising in turbulence measurements, especially of high intensity, to adhere to the method suggested by the expressions developed in Section (3.2) i.e. the residence time weighting. This method should give correct results for two or three dimensional fluctuations of arbitrary high levels of fluctuations as long as the directional effect associated with a minimum number of zero crossings is negligible. This condition can be achieved either by adding periods to the burst by optical frequency shifting or by basing the signal processing of the burst on the available number of fringe crossings. The directional dependence is then reduced to the geometrical cross section of the volume, and the residence time weighting should give correct results independent of the particular shape of the volume even when the volume is truncated by the field of view of the photodetector or by measurements close to a wall.

A number of methods of implementing the residence time correction have been realized. Hösel and Rodi (1977) suggest a circuit, which measures the width at half height of a burst by an analogue method (rectification and low-pass filtering). The method of measuring the total number of fringes in a burst (a digital method, which unlike analogue methods is not frequency dependent) has been adopted by some commercial producers of LDA- equipment. Both the measured number of fringe crossings and the time between the first and last zero-crossing (or the velocity based on the inverse of that time) are made available simultaneously at the output. Experimental evaluation of the residence time correction is still rather scant, but the results of Hösel and Rodi (1977) show good agreement between measured and computed values for mean velocities.

Finally, concerning velocity bias it may be mentioned (as already pointed

out by McLaughlin and Tiederman) that in simultaneous measurement of all three velocity components (or in 2-dimensional measurements in flows in which fluctuations in the third direction are negligible) it is of course possible to compute the magnitude of the velocity vector $\underline{u}_i$, and assign a weighting factor proportional to $|\underline{u}_i|^{-1}$ to each sample set (u_i, v_i, w_i), and even to correct for directional dependence based on the knowledge of the direction of $\underline{u}$. Such correction might be carried out on stored data points after the measurement, but it appears that this method has not yet been tried in actual measurements.

The question of whether other factors influence the data rate is still largely unresolved. Tiederman (1977) raised the question of whether differences in signal-to-noise ratio of fast and slow bursts might influence the data rate. Other physical effects, which cause correlation between data rate and flow velocity include density variations caused by pressure or temperature fluctuations, mixing of fluids with different particle concentration and chemical reactions. Asalor and Whitelaw (1976) derived expressions for the correlation between combustion-induced temperature , pressure , and concentration fluctuation and data rate based on assumptions about the velocity-temperature and velocity-pressure correlations in a diffusion flame. From the analysis and subsequent measurements the authors concluded that in this particular flow the bias effects due to velocity fluctuations confirmed the hypothesis about the velocity-data rat correlation of McLaughlin-Tiederman. Velocity-pressure and velocity-temperature correlation effects were found to be negligible. Reference II discusses briefly the extension of the arguments of Section (3-2) to flows with density fluctuatio

3.5 Correlation and Spectral Measurements

The measurement of covariance functions and spectra plays an important role in turbulence research. These functions reveal the inner structure of the turbulent motion and shed light on the dynamic processes of momentum and energy transfer between the spectral components of the fluctuating velocity.

The experimental and computational methods for the determination of covariance functions and spectra have undergone considerable changes during the last decades in step with the technological development of measuring apparatus and computing facilities. These technical developments include digital sampling and data storage techniques allowing long-time averaging without drift problems, decreasing cost and increasing speed of digital computers, and the development and implementation of more sophisticated computational methods. The latest step in this on-going process is the development of integrated, hybrid analog/digital circuits allowing fast, inexpensive implementation of complex computational methods and transforms. Previous analog delaying and multiplying operations are replaced by digital manipulation of discrete-time samples of the signal. Tradition and computational efficiency have in nearly all cases dictated periodic sampling, but mathematical examinations carried out in the fifties and sixties on the effects of random sampling and the realization that certain forms of random sampling have advantages in spectral computation (e.g. alias-free spectra) plus the fact that the burst type LDA signal processor provides data at random times corresponding to the random arrival of scattering particles in the measuring volume,have brought renewed interest and new developments in random sampling spectral estimation.

Methods of spectrum computation of regularly sampled signals from continuous LDA-signal processors are essentially identical to those used in hot-wire data analysis and the results are derived identically except for the effects of drop-out and ambiguity noise described in Chapter (2). Three basic methods of discrete power spectrum estimation exist:

1) the Blackman-Tukey method based on the Fourier Transform of the autocovariance function,

2) the direct formation of the power spectrum from Fourier transform coefficients of the sampled data, and

3) the digital filter or complex demodulation method.

Many variations exist, and the optimum choice of time lag, sample size and possible smoothing window depends on the type of spectrum expected and the desired characteristics of the resulting estimate.

Consider a record of length T consisting of N samples $[u(t_i)](i=1,2,---,N)$ where t_i is the time of measurement of the i^{th} sample, and let us designate by $C(\tau)$ and $S(\omega)$ the time autocovariance function and spectrum of the underlying continuous signal. The basic characteristics describing the performance of a spectrum estimate are then the deviation of the expected value of the spectrum estimate $\hat{S}(\omega)$ from the true value, i.e. the bias given by

$$B = \hat{S}(\omega) - E[S(\omega)] \tag{3.5.1}$$

where E[ ] denotes mathematical expectation, and the variability given as an expression for the variance of a given estimate, e.g.

$$\text{var}\,[\hat{S}(\omega)] = E[(S(\omega) - E[\hat{S}(\omega)])^2] \tag{3.2.5}$$

These parameters are normally functions of the desired spectral resolution or bandwidth B and the number of samples N.

The effect on spectral aliasing of various forms of random sampling was studied by Shapiro and Silverman (1960), who concluded that although not all types of randomness in the sampling procedure lead to alias-free spectra, many sampling distributions exist, including the Poisson distribution, which will remove aliasing in computed spectra irrespective of the average data rate, albeit at the cost of increased variability. A number of spectral estimates, equivalent to the Blackman-Tukey methods, but based on randomly sampled data, were presented at the 1974 Purdue Workshop on laser anemometry (Thompson and Stevenson 1974). In these methods an estimated autocovariance function was formed from the measured values of velocity $u(t_i)$ and the time increment since the last validated sample, $t_i - t_{i-1}$. The time axis was divided into M slots of equal width $\Delta\tau$, where $\Delta\tau$ is selected to give an effectiv

spectral resolution $\Delta\omega=1/(2n\Delta\tau)$ in the computed spectrum. An estimate of the autocovariance function at $n\Delta\tau$ was formed by adding cross products between samples $u(t_i)$ and $u(t_j)$ separated by lag times t_i-t_j falling in the range $n\,\Delta\tau \pm (1/2)\,\Delta\tau$ and counting the number of such products:

$$C(n\Delta\tau) = \frac{\sum_{i,j} u(t_i)\,u(t_j)}{\sum_{i,j}} \; ; \; (n-1/2)\Delta\tau < t_i - t_j < (n+1/2)\Delta\tau \qquad (3.5.3)$$

The denominator is simply the number of products in the window. The spectrum was then obtained from the autocovariance estimate in the usual manner by Fourier transform after application of a suitable data window, $D(n\Delta\tau)$:

$$\hat{S}_1(\omega_k) = \sum_{n=1}^{M} C(n\Delta\tau)\, D(n\Delta\tau)\, e^{i\,\omega_k\, n\Delta\tau} \qquad (3.5.4)$$

The properties of this spectral estimtor were analyzed by Gaster and Roberts (1975). First a more direct spectral estimator using all occurring lag times $t_i - t_j$ was investigated:

$$\hat{S}_1(\omega) = \frac{1}{\pi\nu^2 T} \sum_{i}^{N} \sum_{i<j}^{N} D(t_i-t_j)\, u(t_i)\, u(t_j) \cos\omega(t_i-t_j) \qquad (3.5.5)$$

This estimator treats each cross product $u(t_i)\,u(t_j)$ as a realization of the autocovariance function for a lag $\tau = t_i-t_j$. Note, zero lag products do not occur. The spectral estimator $S_2(\omega)$ was shown to be consistent and unbiased and to have a variance given by:

$$\mathrm{var}[\hat{S}_2(\omega)] = \frac{3\tau m}{4T}\left[S(\omega) + \frac{\sigma^2}{2\pi\nu}\right]^2 \qquad (3.5.6)$$

where a Poisson sampling process of mean rate ν and a Gaussian random process of mean square velocity σ^2 were assumed. This expression shows the increased variance introduced by the Poisson sampling; the penalty for the random sampling becomes appreciable for mean sampling rates lower than the corresponding Nyquist rate for regularly sampled data.

The spectral estimator (equation 3.5.5) is impractical to implement because of the double summation, but Gaster and Roberts did implement the time-slot approximation (equation 3.5.3), and showed using simulated signals that the variance of the former (equation 3.5.6) is still a reasonable estimate for the variability of the latter. For constant slot width the spectrum is conveniently computed via the FFT, but computation by direct implementation of equation (3.5.3) for logarithmically spaced slots is not unreasonable, since a high frequency estimate at ω_r does not require summing over the full array of covariance values, but only for lags shorter than $1/\omega_r$.

The special features of these spectral estimators may be summarized:

1) no aliasing in the computed spectrum (a fact related to the LDA - method of sampling, not to the particular spectral estimator).

2) reasonably simple implementation, even for non-uniform lags,

3) insensitivity to added white noise due to the fact that only non-zero lag products are used in the estimator, and finally,

4) an increased variance of the spectral estimate relative to regularly sampled signals.

In a more recent paper, Gaster and Roberts (1977) examine a direct transform of the sampled data:

$$\hat{S}_3(\omega) = \frac{1}{2\pi\nu^2 T}\left[\left|\sum_i u(t_i)\, e^{i\omega t_i}\right|^2 - \sum_i u^2(t_i)\, D^2(t_i)\right] \qquad (3.5.7)$$

This estimator is identical in form to the estimator used for regularly spaced samples. However, in this case the time increments are random and the terms in the sum are evaluated at the random sampling times t_i.

However, all samples are weighted equally and the factor $t_i - t_{i-1}$ originally multiplying each term is replaced by the average interval between samples $1/\nu$ and pulled outside the sum. It is shown that the variability of this

estimator, evaluated for Poisson sampling and assuming a Gaussian random process u(t), in general depends on the shape of the spectrum $S(\omega)$, the window D(t) and the length of the record length T but for large record length, approaches the value

$$\text{var}\,[\hat{S}_3(\omega)] = [S(\omega) + \frac{\sigma^2}{2\pi\nu}\,]^2 \qquad (3.5.8)$$

The first term represents the variability of the conventional periodogram with periodic sampling, whereas the second represents the added variability due to the random sampling. Data smoothing windows or block averaging may be applied to form stable spectrum estimates. Gaster and Roberts suggest that in many cases it will be advantageous to use a spectral bandwidth which increases in proportion to the center frequency of the estimate in order to obtain stable estimates at high frequencies.

So far only the slotted time lag autocovariance method has been applied to actual burst LDA realizations (no residence time weighting). Measurements were reported at the 74 Purdue meeting by Smith and Meadows and by Scott. These measurements were in free jets in air. Other tests included measurements of acoustical vibrations with a loudspeaker. The basic feasibility of the burst type LDA power spectrum measurement was proven. Later results have been reported by Mayo et al (1974) and by Bouis et al (1977. None of these measurements made any attempt to correct for the bias effects discussed in Section 3.2.3 and below.

It seems that more experience with LDA spectral measurements are needed before all aspects of error sources are clarified. A study (Wang 1976, and Asher, Scott and Wang 1974) of various sources of errors in relation to counter LDA data concludes that the quantizing of the output due to the finite resolutio of the counter itself is the greatest source of error in LDA single burst spectral measurements. However this analysis did not consider the "apparent turbule caused by the finite dimensions of the measuring volume in the presence of grad-

ients within the volume as described in Section 3-2 nor did it consider the biasing effects introduced by using uncorrected data. It should be apparent that bias effects will somehow modify the computed spectral estimator as well as mean and mean square values, and that bias correction methods should be applied to spectral measurements as well.

In Section (3-2), it was shown that autocorrelation from burst processors could be computed correctly without bias as

$$R(\tau) \simeq \frac{\sum_{i,j} u_i\, u_j\, \Delta t_{ij}}{\sum_{i} \Delta t_{ij}}; \qquad \tau = |t_i - t_j| \tag{3.5.8}$$

where Δt_{ij} is the amount of time a realization u_i with residence time Δt_i at t, overlaps another realization u_j of residence time Δt_j at $t_j = t_i + \tau$. Recall that self products (i=j) are not included in the sum since they result in the unwanted spike at the origin. This value (τ=0) is computed separately by equation (3.2.16).

In practice, equation (3.5.8) is not a useful algorithm since not only must the particle velocities and transit times be stored but also their arrival times from which the overlap is computed.

It can be shown (Buchhave, 1978) that an estimator which retains the essence of equation (3.5.8) can be formed by simply multiplying each velocity realization taken at different times (or from different records) by its residence time and dividing by the sum of the residence times:

$$R'(\tau) = \frac{\sum_{i,j} u_i\, u_j\, \Delta t_i\, \Delta t_j}{\sum_{i,j} \Delta t_i\, \Delta t_j}; \qquad \tau = |t_i - t_j| \tag{3.5.11}$$

This estimator is not biased due to velocity - data rate correlation, if angle effects have been minimized by frequency shift or similar techniques (c.f. the discussion about bias correction in Section (3-2). It is also easy to see that this non-biased algorithm can be fitted directly into the time slot approximation discussed earlier.

To this point it appears that the significance of the bias correction in the formation of autocorrelation functions and spectra has not been studied. This question will be taken up in a succeeding publication (Buchhave, 1978). All attempts to-date to reconstruct the autocorrelation from burst LDA's have been biased since no attempt has been made to correct for the residence time (or particle arrival rate).

Some preliminary results were published at the 1978 Purdue meeting (Buchhave, 1978a) and the question will be treated in more detail in a succeeding publication (Buchhave, 1978b).

4. REFRACTIVE INDEX EFFECTS ON LDA MEASUREMENT

4.1 Source and Magnitude of Refractive Index Fluctuations

If the laser beams of the LDA must propagate through a medium having random index of refraction fluctuations, the ray paths will no longer be straight, but will have random fluctuating curvature, and the phase and amplitude of the arriving signal will fluctuate randomly. This is the phenomenon which causes jitter and scintillation of stellar images, and scintillation of extra-terrestrial radio sources, where the index of refraction fluctuations are due primarily to temperature fluctuations in the atmosphere. There is an extensive literature on this subject (see, for example, Monin & Yaglom 1975, Chapter 9).

The effect of index of refraction fluctuations on LDA measurements has been considered by Lumley et al (1978), whom we follow closely. These fluctuations arise primarily from fluctuations of temperature or composition when the LDA is used in flows in which heat transfer, chemical reactions or combustion are taking place. We will find in section 4.3 that fluctuations of the order of 2×10^{-6} are necessary for an appreciable effect. Let us consider what level of fluctuations might be met under various circumstances. In gases, the index is usually given for Sodium light (λ = 0.5893 μm), and at 273° K and one standard atmosphere (101 kNm^{-2}). The index under other conditions is approximately proportional to density and is only a weak function of wavelength in the visible range. Some representative values of $(n-1)10^4$ under standard conditions are:

CH_4: 4.44	O_2: 2.71
CO_2: 4.48	H_2O: 2.49

Air: 2.93

(Handbook of Chemistry & Physics, p. E-224). Taking air as an example, we can write

$$(n-1)10^4 = 2.93 \frac{273}{101x10^3} \frac{p}{T} = 7.92 \times 10^{-3} \frac{p}{T} \qquad (4.1.1)$$

where p is absolute pressure in Nm^{-2} and T is absolute temperature in ^oK. If we consider isentropic variations in the pressure in a compressible flow, and make use of a quasi-Gaussian estimate relating pressure and velocity fluctuations (Batchelor, 1956, p. 182), we find that r.m.s. velocity fluctuations of the order of 70 m/s are necessary to produce index of refraction fluctuations of the necessary level. Since this corresponds to a 4% turbulence level in a sea-level mean flow at Mach 5, we can usually neglect this source of refractive index fluctuations, and take P = const. For temperature fluctuations we can write

$$n' = - (n-1)_o \frac{T_o}{T^2} \theta \qquad (4.1.2)$$

where T_o and $(n-1)_o$ are the values at 273^oK, and θ is the temperature fluctuation. Thus, for air at 273^oK, $dn/d\theta = -1.07x10^{-6}\ ^oK^{-1}$ while at 1300 ^oK $dn/d\theta = -4.73x10^{-8}\ ^oK^{-1}$.

As far as composition fluctuations are concerned, to a first approximation we may take the deviation proportional to the relative mass fraction X. Thus, for a two component mixture, we obtain

$$dn/dX = n_1 - n_2 = (n_1 - n_2)_o \frac{T_o}{T} \qquad (4.1.3)$$

Considering, for example, a Methane-Oxygen mixture, we have $dn/dX = 1.73x10^{-4}$ at 273 °K, and $3.63x10^{-5}$ at 1300 °K. Since we may have mass fraction fluctuations of order unity, these are also representative of the values of n'.

In liquids, the index of refraction is considerably more sensitive to temperature. In water, for example, at 273 °K, we have $dn/d\theta = -9x10^{-5}\ ^oK^{-1}$

for the absolute index of refraction for sodium light (Handbook of Chemistry & Physics, p. E-223).

In addition, since the refractive index of various liquids differs usually in the first decimal, mixing of two liquids of differing indices can result in values of dn/dX of order 10^{-1}; glycerine-water results in 0.14, for example. If we consider the case of sea water (Handbook of Chemistry and Physics, p. D-249) we find the index of refraction to be primarily a function of salinity (measured in parts per million), with $dn/dS = 1.8 \times 10^{-4}$. If the LDA were used in an experiment involving the mixing of sea water at $30°/_{oo}$ salinity and fresh water, we could have values of n' of the order of 5.4×10^{-3}.

It is evident that there are a number of situations in which the LDA could be used in which substantial index of refraction fluctuations might be present; we must examine the sensitivity of the measurements to these fluctuations.

4.2 Effect of Fluctuations on Ray Path and Phase in the Geometrical Optics Limit.

We may assume that the wavelength of the radiation is short relative to the size of the inhomogeneities, and that the radiation is monochromatic. We may then go to the geometrical optics limit (see Tatarski, 1961, section 6.1; Neubert, 1970). If k is the wavenumber of the radiation, and n the index of refraction, if we write $E = A\exp[iS]$, where E is any component of the electric field, A is the amplitude and S is the phase, we obtain the eikonal equation for the phase

$$S_{,i}\ S_{,i} = k^2 n^2(\underline{x}) \tag{4.2.1}$$

From the canonical Hamiltonian solution to the eikonal equation (Kravtsov, 1968) we obtain

$$S = S_o + k \int_o^S n(S')\, dS' \tag{4.2.2}$$

where the integral is taken along the ray path $X_i(S)$ given by the Fermat relation

$$m_{,i} = \frac{d}{ds}\left(n \frac{dX_i}{dS}\right) \tag{4.2.3}$$

It is probably easiest to consider the fringe mode of operation, in which two beams (in the undisturbed state)

$$\begin{aligned} \underline{k}^{(i)}&: (k \sin \theta/2,\ k \cos \theta/2, 0) = k\underline{i} \\ \underline{k}^{(r)}&: (-k \sin \theta/2,\ k \cos \theta/2, 0) = k\underline{r} \end{aligned} \tag{4.2.4}$$

form fringes which, if undisturbed, would lie stationary in planes perpendicular to the x_1 axis. Lines of constant phase difference of the two signals will be lines of constant fringe phase. If these lines of constant fringe phase move with a certain velocity, this will produce an error in the apparent particle velocity.

We may calculate

$$\frac{dS}{dt} = k \int_0^S \dot{m}(s')ds' + k\, u(s) \frac{dS}{dt} \tag{4.2.5}$$

where $\frac{dS}{dt} = \frac{\partial S}{\partial X_i} \frac{dX_i}{dt}$. To hold the phase difference constant, we must allow x_1 to vary, corresponding to the fringe velocity. Hence, dX_1/dt will consist of two parts, $\frac{\partial X_1}{\partial t} + \frac{\partial X_1}{\partial \xi_1} \frac{d\xi_1}{dt}$ where ξ_1 is the co-ordinate of the ray on the initial wave front. We are not interested in the motion of $\underline{\xi}$ however, but in the motion which it produces at the scattering volume, so that we can write $\frac{dX_1}{dt} = \frac{\partial X_1}{\partial t} + u_1$, where u_1 is the velocity of the fringe pattern. Hence

$$\frac{d}{dt}\left(S_{(i)} - S_{(r)}\right) = 0 = k\left(\int_{(i)} \dot{n}(s)ds - \int_{(r)} \dot{n}(s)ds\right)$$

$$+ kn\left[\left(\frac{\partial X_j^S}{\partial t} + u_j\right)\left(\frac{\partial S^{(i)}}{\partial X_j} - \frac{\partial S^{(r)}}{\partial X_j}\right) + \frac{\partial X_j^D}{\partial t}\left(\frac{\partial S^{(i)}}{\partial X_j} + \frac{\partial S^{(r)}}{\partial X_j}\right)\right] \tag{4.2.6}$$

where $\partial X_j^S/\partial t$ is 1/2 the sum of the ray terminal velocities and $\partial X_j^D/\partial t$ is 1/2 the difference. We have selected rays which intersect instantaneously, so that the values of n at the end of each ray are the same. We may now consider $n = \bar{n} + n'$, $n' << \bar{n}$. The first term in (4.2.6) is of order n', and it is clear that $\partial X_j/\partial t + u_j$ is at most of order n'. Hence, to lowest order we can neglect the departure of n and $\frac{\partial S^{(i)}}{\partial X_j} - \frac{\partial S^{(r)}}{\partial X_j}$ from their undisturbed values; we may also take the integrals in (4.2.6) along the undisturbed rays. In addition, we take the termination of the rays on a plane perpendicular to the x_2 axis, passing through the point of intersection of the undisturbed rays. Hence, $X_2 = x_2$, a fixed value, and the second term in square brackets in (4.2.6) vanishes. Since for the undisturbed rays we have $\partial s/\partial X_j = k_j/k$, we can write

$$u_1 = -\frac{\partial X_1^S}{\partial t} - \frac{1}{\bar{n}\, 2 \sin\frac{\theta}{2}} \left(\int_0^L \dot{n}\, (\underline{x} \cdot \underline{i}) ds - \int_0^L \dot{n}\, (\underline{x} \cdot \underline{r}) ds \right) \tag{4.2.7}$$

where we have taken the undisturbed rays to be of equal length L.

To evaluate $\partial X_1^S/\partial t$, we must integrate (4.2.3) twice, making use of the assumption that n' is small. To first order we obtain

$$\frac{\partial X_1}{\partial t} = \frac{L}{\bar{n}} \int_0^L (1-\frac{S}{L})\, \dot{n}_{,1} ds \tag{4.2.8}$$

where we are neglecting the change in slope from the undisturbed value as the ray pierces the plane, a term of order $L \frac{n'}{\bar{n}} \sin\frac{\theta}{2}$, which is considerably smaller. Thus,

$$u_1 = -\frac{1}{2}\frac{L}{\bar{n}} \left(\int_0^L (1-\frac{S}{L})\, \dot{n}_{,1} (\underline{x}\cdot\underline{L}) ds + \int_0^L (1-\frac{S}{L}) \dot{n}_{,1} (x\cdot r) ds \right)$$

$$- \frac{1}{\bar{n}\, 2 \sin\frac{\theta}{2}} \left(\int_0^L \dot{n}(x\cdot i) ds - \int_0^L \dot{n}\, (\underline{x}\cdot\underline{r}) ds \right) \tag{4.2.9}$$

Physically, it can be seen what is happening: presuming that the phases stay the same, if the beams swing in the same direction, the fringes will

move with them. If the beams swing in opposite directions, however, the fringes will remain stationary. In addition, if the relative phases change, the fringes will move. We may note that one of the standard techniques for examining flows without mean velocity is to shift the frequency of one beam to produce a steady drift of the phase difference, and hence of the fringes. To produce this effect, the parenthesis of the second term in (4.2.9) is replaced by $\Delta\omega/k$.

The ratio of the first and second terms can be estimated by taking $n_{,1} = n'/\lambda_n$, $\dot{n} = n_{,1} U = n'U/\lambda_n$ where λ_n is the Taylor microscale for the index of refraction fluctuations. The ratio is $L \sin\frac{\theta}{2}/\lambda_n$. Since $\sin\frac{\theta}{2} \sim 0.1$ in most situations, and L will usually be at least 3ℓ, the integral scale, we have $0.3\sqrt{R_\ell/15}$ for the ratio, where $R_\ell = u\ell/\nu$. If $R_\ell = 167$, the terms are comparable; if $R_\ell = 1500$, the terms differ by half an order of magnitude. Laboratory values of R_ℓ typically lie between these two values, so that although the first term is probably larger in most circumstances, it probably does not always dominate. It is of course true also that path length and scattering angle will differ in different experimental situations.

What is not apparent from (4.2.9) however, is that the spectra of the two terms differ markedly. Lumley et al (1978) find that while the spectrum of the first term rises sharply as $K^{4/3}$, that of the second falls as $K^{-2/3}$, so that the contaminating effect at the high end of the spectrum is felt from the first term long before that from the second term. This is because the first term depends on derivatives of the index of refraction field one order higher than are present in the second. We will limit our consideration to the first term, and refer the reader to Lumley et al (1978) for a discussion of the second.

4.3 Beam Swinging Effects.

It is relatively straightforward to show that the cross-spectrum between

the two beam-swinging terms in (4.2.9) is negligible for large L, since the region of correlation is of fixed extent as the beams diverge. Thus, the spectrum can be written as

$$\frac{1}{4}\frac{L^2}{\bar{n}^2} U^2 \, 2\pi L k_1^4 \int_{-\infty}^{+\infty}\int \left[\delta(\underline{k}\cdot\underline{i}) + \delta(\underline{k}\cdot\underline{r})\right] S_n(\underline{k}) dk_2 dk_3 \tag{4.3.1}$$

where $K_1 U = \omega$ *. Taking the spectrum of index of refraction fluctuations to be isotropic, so that $S_n = E_n(k)/4\pi k^2$, where $E_n(k)$ is the three-dimensional spectrum, and

$$E_n = 3 \frac{\overline{n'^2}}{\overline{q^2}} \bar{\varepsilon}^{2/3} K^{-5/3} \tag{4.3.2}$$

which is a reasonable approximation for any scalar (Monin & Yaglom, 1975, section 23.5) we obtain for the spectrum

$$\frac{2\pi}{15} \frac{\overline{n'^2}}{\bar{n}^2} \frac{L^3 U^2}{\ell^2} \left[\cos\frac{\theta}{2}\right]^{8/3} (k,\ell)^{4/3} \tag{4.3.3}$$

For this spectrum to rise to the same value as the ordinary one-dimensional velocity spectrum at the highest end, $K_1\eta = 0.55$ (Tennekes & Lumley, 1972, p. 273 requires

$$\frac{n'^2}{\bar{n}^2} = 3.52 \left(\frac{u}{U}\right)^2 \left(\frac{\ell}{L}\right)^3 R_\ell^{-9/4} \left[\cos\frac{\theta}{2}\right]^{-8/3} \tag{4.3.4}$$

If we take typical values of $u/U \sim 10^{-2}$, $L/\ell \sim 3$, $R_\ell \sim 800$, $\cos\frac{\theta}{2} \sim 1$, we have $n'/\bar{n} = 1.96 \times 10^{-6}$ required.

This value of $n'/\bar{n}$ corresponds to temperature fluctuations of 1.83 °K in air at 273 °K, or to fluctuations of 41 °K in air at 1300 °K, We may consequently expect this to be a significant effect in combustion. Methane-Oxygen mass fraction fluctuations of 5.39×10^{-2} at 1300 °K are also sufficient

* and we have used Taylor's hypothesis; that is, we have assumed that the principal source of variation contributing to the time derivatives appearing in (4.2.9) is the convection of the frozen index-of-refraction fluctuations across the ray path, and we have taken the mean velocity in the 1-direction.

to produce these levels of $n'/\bar{n}$. Note that the cut-off point, where (4.3.3) crosses the velocity spectrum, goes as $(n'/\bar{n})^{2/3}$; hence, nearly a full decade will be lost when the mass fraction fluctuations of CH_4-O_2 are O(1) at 1300 °K. In addition, it must be noted that at the cross-over point the combined spectrum is twice the value of either, so that the spectrum is contaminated by 10% or more down to a wavenumber about half the cross-over value.

In water, of course, the situation is much more serious: 2.17×10^{-2} °K will satisfy (4.3.4), and 1 °K will cause loss of a decade.

Note that the spectral level goes up quite rapidly as L increases, every effort should be made to keep L as small as possible, though it will probably not be possible to reduce it much below a value of 3.

Using the spectrum (4.3.3), we can integrate to find the r.m.s. value of the spurious velocity. This is useful because in many experimental situations a continuous signal is not obtained, so that the spectral information is not available. Hence, only the direct influence on the variance can be determined. Integrating (4.3.3) we obtain

$$\left(\frac{\partial X_1^S}{\partial t}\right)^2 = 8.90\times10^{-2}\,\frac{\overline{n'^2}}{\bar{n}^2}\,\left(\frac{L}{\ell}\right)^3 U^2 R_\ell^{7/4}\,\left(\cos\frac{\theta}{2}\right)^{8/3} \qquad (4.3.5)$$

If we adopt as a criterion that the r.m.s. value of the spurious velocity should be 10% that of the real velocity, then this requires that

$$\frac{\overline{n'^2}}{\bar{n}^2} = 0.112\,\left(\frac{\ell}{L}\right)^3\left(\frac{u}{U}\right)^2 R_\ell^{-7/4}\,\left(\cos\frac{\theta}{2}\right)^{-8/3} \qquad (4.3.6)$$

Again using the values cited below (4.3.4), we find a level of $n'/\bar{n} = 1.86\times10^{-6}$ required, or virtually the same as that arising from the criterion (4.3.4). Hence, in this parameter range, a signal/ noise ratio of unity at the high end of the spectrum or 10% contamination of the r.m.s. value of the signal, are equivalent.

We should also estimate the r.m.s. motion of the ray terminus, since this represents an uncertainty in the particle location; in addition, if the motion of the ray terminus becomes too large, it is possible for the beams to fail to overlap, and thus produce no fringes. In this case, the signal is lost. It is simplest to write (4.2.3) on coordinates along and perpendicular to the undisturbed ray path. Then, making the same assumptions, we obtain

$$\overline{X_1^2} = \frac{\pi}{2}\left(\frac{3}{2}\right)^{1/2} \frac{\overline{n'^2}}{\bar{n}^2} \frac{L^3}{\ell} \left(\frac{2}{3} R_\ell^{1/4} - 1\right) \qquad (4.3.7)$$

Taking the same values quoted below (4.3.4) we obtain $\sqrt{\overline{X_1^2}} \sim 0.5\mu m$, or $5\mu m$ at ten times the level of $n'/\bar{n}$. These small values are quite consistent with the fact that the velocities of the fringes occur primarily at the highest frequencies. If $\sin\frac{\theta}{2} \sim 0.1$, a typical value, the fringe spacing is roughly $2.5\mu m$, if light of wavelength $0.5\mu m$ is used. Thus, we are envisioning r.m.s. motion of between 20% and 200% of the fringe spacing. The beam diameter at the scattering volume is usually of order 10 fringes, or $25\mu m$. It is clear that only under extraordinary circumstances would $\sqrt{\overline{X_1^2}}$ be large enough for the beams to fail to intersect. However, if we consider the case of mixing of sea water at $30^\circ/_{oo}$ salinity with fresh water, we obtain $\sqrt{\overline{X_1^2}} \sim 1.24$ mm, which is more than sufficient.

4.4 The Possibility of Correction

Correction of the measurements for these effects is possible in several ways. Obviously, if the spectrum can be measured sufficiently beyond the cross-over point to reach a region of approximate $K^{4/3}$ dependence, this can be subtracted. In the absence of this, however, there are other possibilities. If one beam can be passed through the same part of the flow and heterodyned with an unscattered beam, and the result processed by a detector, then from

(4.2.5) we get a direct measure of

$$kU \int_0^L n_{,1}\, ds \tag{4.3.8}$$

(assuming Taylor's hypothesis). This will have a spectrum given by

$$\frac{4\pi}{15} k^2 \overline{n'^2} L U^2 (\cos \tfrac{\theta}{2})^{8/3} (k,\ell)^{-2/3} \tag{4.3.9}$$

and a variance given by

$$6{\cdot}11\ K^2 \overline{n'^2} \frac{L}{\ell} U^2 (\cos \tfrac{\theta}{2})^{8/3} (\tfrac{2}{3} R_\ell^{1/4} - 1) \tag{4.3.10}$$

Depending on the experimental situation, the value of L may not be the same. However, if the various parameters can be estimated, an estimate for $\overline{n'^2}$ can be obtained from either (4.3.9) or (4.3.12) and this used to correct the measurements.

5. PARTICLE PROBLEMS

5.1 Criteria for Particle Selection

We cannot consider here the various types of particles commercially available for flow seeding. We will consider, however, the criteria which should be used for particle selection.

The basic requirement is that the particles follow the fluid motion down to the smallest scale of interest. We will presume here that the smallest scale of interest is $1/\eta$ where η is the Kolmogorov microscale; this corresponds to $k\eta=0.55$, where k is wavenumber. This is essentially the viscous cut-off (see Tennekes & Lumley, 1972, p. 270). By following the fluid motion, we mean that the value of the spectrum of particle/fluid relative velocity should be small compared to the value of the spectrum of fluid velocity at the wavenumber in question. Following Lumley (1976), and taking the fluid velocity seen by the particle to be essentially the Langrangian velocity, we have

$$\frac{a_1^2\,\omega^2}{1+a_1^2\,\omega^2} \ll 1 \qquad (5.1.1)$$

for $\omega = 0.74\ v/\eta$. a_1 is the particle time constant, and $v = (\nu\varepsilon)^{1/4}$ the Kolmogorov velocity. If we take as a specific criterion that the velocity should be in error by no more than 1%, we may write

$$a_1\omega \leq 10^{-2} \qquad \text{or} \qquad a_1\left(\frac{\varepsilon}{\nu}\right)^{1/2} \leq \frac{1}{74} \qquad (5.1.2)$$

Using $\varepsilon = u^3/\ell$ (Tennekes & Lumley 1972, p. 68), we may write (5.1.2) as

$$a_1 \frac{u}{\ell} R_\ell^{1/2} \leq \frac{1}{74} \qquad (5.1.3)$$

In a turbulent pipe flow of water at 1 m/s, diameter 6 cm, this gives roughly

$a_1 \leq 2\times10^{-4}S$; for the same flow in air we have $a_1 \leq 9\times10^{-4}S$. We may use the Stokes form for a_1 (Lumley, 1967):

$$a_1 = \frac{d^2}{36\nu}\left(2\frac{\rho_r}{\rho_f} + 1\right) \qquad (5.1.4)$$

where ρ_r is the particle density and ρ_f that of the fluid, and d is the particle diameter. For use in air it is difficult to find particles of density much less than 1 g/cc For such particles, the value of $a_1 = 9\times10^{-4}S$ corresponds to d ~ 17μm. For the case of water, if we presume that ρ_r is still 1 g/cc, we have d ~ 49/μm.

Since scattering particles typically in use have diameters of the order of a few microns, we may be sure that in these typical situations there is no need for concern that the particles are not following the flow. It is not hard to think of situations with higher Reynolds numbers and shorter characteristic times, however (e.g.- rocket exhausts) where this might be a problem.

5.2 Influence of Non-Uniformities of Particle Concentration

Two common seeding methods are likely to produce non-uniformities of particle concentration which can influence velocity statistics. In one, a point source of particles is introduced upstream of the measurement location; in the other, only the turbulent part is seeded, in a turbulent flow having a turbulent/non-turbulent interface.

Let us consider first the case of a point source. For simplicity we will take a homogeneous turbulence with a uniform mean velocity U. To simplify matters further, we can suppose that the particles are released along a line perpendicular to the flow, parallel to the x_3 axis, a distance L upstream. In this way we need consider only wandering of the particles in the x_2 direction. The generalization from a line source to a point source is straightforward. Now, if the particles are released along the x_3 axis between $-dx_2/2 \leq x_2 \leq dx_2/2$ at $x_1 = 0$, and measurements are carried out along

the line $x_1 = L$, $x_3 = 0$, we will have a signal if $X_2(L, x_2, 0, t|t-L/0) \varepsilon[-dx_2|2, +dx_2|2]$, where $X_2(\underline{x}, t|t')$ is the 2-position at t' of the material point which was or will be at $\underline{x}$ at t (we are ignoring dispersion in the direction of the mean flow). If, for simplicity, we suppose that the turbulence is Gaussian, then X_2 and $u_2(\underline{x},t)$ will be jointly Gaussian. We have

$$X_2(L,x_2,0,t|t-L/U) = x_2 + \int_t^{t-L/U} u_2(X(\underline{x},t|t'),t')dt' \tag{5.2.1}$$

The mean value is $\overline{X_2} - x_2$, and the variance is

$$\overline{(X_2-x_2)^2} = 2\,\overline{u_2^2}\,T_L\,L/U = \sigma_2^2, \text{ say} \tag{5.2.2}$$

where T_L is the Lagrangian integral time scale, and we have presumed that L/U is at least several times T_L, a restriction probably not met in practice. For the cross-correlation, we may write

$$\overline{u_2(\underline{x},t)(X_2(\underline{x},t|t-L/U)-x_2)} = \overline{u_2^2}\int_t^{t-L/U} \rho_L(t'-t)\,dt' \simeq -\,\overline{u_2^2}\,T_L \tag{5.2.3}$$

where ρ_L is the Lagrangian autocorrelation coefficient. Hence, the autocorrelation coefficient is given by

$$\rho = -\sqrt{\frac{T_L U}{2L}} \tag{5.2.4}$$

The probability density for $-dx_2/2 < X_2 \leq +dx_2/2$, and the joint densities for u_2 to have an arbitrary value while $-dx_2/2 < X_2 \leq +dx_2/2$ may be written down immediately, from which we obtain the conditional probability for u_2, given that $X_2(L,x_2,0,t|t-L/U) \varepsilon [-dx_2/2, +dx_2/2]$:

$$\left[\frac{1}{\sqrt{2\pi}\,\sigma_1\sqrt{1-\rho^2}}\exp\left[\left(-\frac{1}{(1-\rho^2)}\,\frac{u_2}{\sigma_1} + \rho\,\frac{x_2}{\sigma_2}\right)^2\right]\right] \tag{5.2.5}$$

If the option is taken, that the processor holds the last value during drop-outs (see section 2.7), then the probability density for the total signal is the same as that for the signal during the on-times. Thus, (5.2.5) will be the density for the total signal. We see that, if the measurement point is not directly downstream of the release point, a spurious mean velocity will be introduced, given by

$$\overline{u_2} = -\rho \frac{\sigma_1}{\sigma_2} x_2 = + x_2 \, U/2L \tag{5.2.6}$$

while the variance is reduced:

$$\overline{u_2^2} \, (1-T_L U/2L) \tag{5.2.7}$$

even directly downstream of the release point. One can conceivably get sufficiently far downstream so that $T_L U/2L \ll 1$, so that the effect is negligible, but this is often beyond the range of the experiment. Roughly speaking, $T_L = \ell/3u$ (Tennekes & Lumley, 1972, p.278), so that

$$\frac{T_L U}{2L} \simeq \frac{1}{6} \frac{U}{u} \frac{\ell}{L} \tag{5.2.8}$$

Since U/u is probably between 10 and 10^2, for an error of no more than 10% in the velocity variance, we require $L/\ell \leq 17$ or 170 respectively; that is of the order of 10-10^2 boundary layer thicknesses, jet diameters, etc.

The second seeding method which can cause problems concerns uniform seeding of the turbulent part of a flow. For example, if a jet is uniformly seeded at the nozzle exit, then downstream the seeded material will correspond exactly with the turbulent fluid, and there will be no seeding in the non-turbulent part exterior to the turbulent/non-turbulent interface. If the processor holds the last value of the signal each time the signal drops out, the probability density of the velocity will be exactly that measured in the turbulent part of the fluid only, which is observed to differ considerably from that measured in both turbulent and non-turbulent parts (Hedley & Keffer,

1974). Since in most flows, intermittancy extends deep into the flow, reaching the centerline in a wake (Townsend, 1956), this is not a useful way to measure overall properties. It is, however, an ideal way to measure properties in the turbulent fluid only, a matter of considerable current interest. Such an application would eliminate the necessity of establishing threshold criteria for the velocity field, always more or less unsatisfactory. The results obtained should be essentially comparable with those obtainable with the hot-wire by conditioned sampling on a temperature signal, if the turbulent fluid is heated.

REFERENCES

Adrian, R.J. and Orloff, K.L. (1977) "Laser Anemometer Signals: Visibility Characteristics and Application to Particle Sizing". Appl. Optics 16: 677-684.

Asalor, T.D. and Whitelaw, T.H. (1976) "The Influence of Combustion-induced Particle Concentration Variations on Laser-Doppler Anemometry". Proceedings of the LDA Symposium Copenhagen 1975: 115-137. Copenhagen: P.O. Box 70, 1740 Skovlunde, Denmark, 736 pp.

Asher, J.A., Scott, P.F. and Wang, J.C. (1974) "Parameters Affecting Laser Velocimeter Turbulence Spectra Measurements". Final Report (AEDC-TR-74-54) Contract No. F40600-72-C-0013, October, 1974.

Baker, R.J. and Wigley, C. (1976) "Design, Evaluation and Application of a Filter Bank Signal Processor". In Proceedings of the LDA-Symposium Copenhagen 1975: 350-363. Copenhagen: P.O. Box 70, 1740 Skovlunde, Denmark, 736 pp.

Batchelor, G.K. (1956) "The Theory of Homogeneous Turbulence, Cambridge, The University Press.

Berman, N.S. and Dunning, T.W. (1973) "Pipe Flow Measurements of Turbulence and Ambiguity Using Laser-Doppler Velocimetry". J. Fluid Mech., 61, pt. 2: 289-299.

Bouis, X, Gourtot S and Pfeiffer, H.T. (1977). "Laser Anemometry: Measurement of the Spectral Power Density of Velocity Variations in Turbulent Flow".ISL-R-126/76 Contract No. DRME-75/055 (B77-32497/86A).

Buchhave, P. (1976) "Biasing Errors in Individual Particle Measurements with the LDA - Counter Signal Processor". In Proceedings of the LDA-Symposium Copenhagen 1975: 258-278. Copenhagen: P.O. Box 70, 1740 Skovlunde, Denmark, 736 pp.

Buchhave, P.(1978a) "Bias Corrections in Turbulence Measurements by the Laser Doppler Anemometer", to be published in Proceedings of the Third Internationa Workshop on Laser Velocimetry, July 11-13,1978. Purdue Univ. W.Lafavette, Ind

Buchhave, P. (1978b)"Errors and Correction Methods in Turbulence Measurement with an LDA". Ph.D. Thesis, Department of Mechanical Engineering, State University of New York at Buffalo.

Drain, L.E. (1972) Coherent and Non-coherent Methods in Doppler Optical Beat Velocity Measurement". J. Phys. D, 5: 481-495.

Durrani, T.S. and Greated, C.A. (1973)"Statistical Analysis and Computer Simulation of Laser Doppler Velocimeter Systems". Trans IEEE, IM-22:23-34.

Durrani, T.S., Greated, C.A. (1977) "Laser Systems in Flow Measurement". New York and London: Plenum Press, 289 pp

Durst, F. and Eliasson, B. (1976) "Properties of Laser-Doppler Signals and Their Exploitation for Particle Size Measurements." In Proceedings of the LDA-Symposium Copenhagen 1975: 457-477. Copenhagen: P.O. Box 70, 1740 Skovlunde, Denmark, 736 pp.

Durst, F., Melling, A., Whitelaw, J.H. (1976) "Principles and Practice of Laser-Doppler Anemometry". New York: Academic Press, 405 pp.

Edwards, R.V., Angus, T.C., Franch, M.J. and Dunning, T.W., Jr. (1971). "Spectral Analysis of the Signal from the Laser Doppler Flowmeter: Time Independent Systems". J. Appl. Phys. 42: 837-850.

Erdman, J.C. and Gellert, R.I. (1976). Particle Arrival Statistics in Laser Anemometry of Turbulent Flow". Appl. Phy. Lett., 29: 408-411.

Farmer, W.M. (1972) "Measurement of Particle Size, Number Density, and Velocity Using a Laser Interferometer". Appl. Optics 11: 2603-2612.

Fog, C. (1976) "A Photon Statistical Correlator for LDA-application. In Proceedings of the LDA-Symposium Copenhagen 1975: 336-349. Copenhagen: P.O. Box 70, 1740 Skovlunde, Denmark, 736 pp.

Gaster, M. and Roberts, J.B. (1975) "Spectral Analysis of Randomly Sampled Signals".J. Inst. Maths. Applics., 15: 195-216.

Gaster, M. and Roberts, J.B. (1977). "The Spectral Analysis of Randomly Sampled Records by a Direct Transform". Proc.R.Soc.Lond.A, 354: 27-58, 1971

George, W.K. (1971), "An Analysis of the Laser Doppler Anemometer and its Application to the Measurement of Turbulence. Ph.D. Thesis, Dept. of Mechanics, The Johns Hopkins University.

George, W.K. (1972), "Limitations on the Measurement of Unsteady Flow Velocities with a Laser Doppler Velocimeter", Fluid Dynamic Measurements in the industrial and medical environment, Leicester Univ.Press, England.

George, W.K. and Lumley, J.L. (1973) "The Laser-Doppler Velocimeter and its Application to the Measurement of Turbulence". J. Fluid Mech., Vol. 60 pt. 2: 321-362.

George, W.K. (1974) "The Measurement of Turbulence Intensities Using Real-Time Laser Doppler Velocimetry". J. Fluid Mech., 66, pt. 1: 11-16.

George, W.K. (1976) "Limitations to Measuring Accuracy Inherent in the Laser Doppler Signal". In Proceedings of the LDA-Symposium, Copenhagen 1975: pp. 20-63. Copenhagen: PO Box 70, 2740 Skovlunde, Denmark, 736 pp.

George, W.K., Buchhave, P., and Lumley, J.C., (1978) "Measuring Turbulence with a Burst Processor Laser Doppler Anemometer". To be submitted for publication, The Physics of Fluids.

Greated, C. and Durrani, T.S. (1971) "Signal Analysis for Laser Velocimeter Measurements". J. Phys. E., 4: 24-26.

Handbook of Chemistry and Physics (R.C. Weast, ed.) 58th Edition (1977-78) CRC Press, Inc., Cleveland, Ohio.

Hanson, S. (1974) "Coherent Detection in Laser Doppler Velocimeters". Opto-electronics, 6: 263-269.

Hedley, T.B. and Keffer, J.F. (1974) "Some Turbulent/Non-Turbulent Properties of the Outer Intermittant Region of a Boundary Layer. J. Fluid Mech., Vol. 64, Part 4; 645-678.

Hösel, W. and Rodi, W. (1977). "New Biasing Elimination Method for Laser Doppler Velocimeter Counter Processing", Rev.Sci.Instru., 48: 910-919.

Karpuk, M.E. and Tiederman, W.G., Jr. (1976) "Effect of Finite-size Probe Volume Upon Laser Doppler Anemometer Measurements AIAA J., 14: 1105-1109.

Kravtsov, Y.A. (1968) "Two New Asympototic Methods in the Theory of Wave Propagation in Inhomogeneous Media"(Review), Sov. Phys. Acoust. Vol. 10, No. 1; 1-17.

Kreid, D.K. (1974). "Laser-Doppler Velocimeter Measurements in Non-uniform Flow: Error Estimates". Appl. Optics, 8: 1872-1881.

Lading, L. (1973) "Analysis of Signal-To-Noise Ratio of the Laser Doppler Velocimeter". Opto-Electronics, 5: 175-187.

Lading, L. and Edwards, R.V. (1976) "The Effect of Measurement Volume on Laser Doppler Anemometer Measurements as Measured on Simulated Signals". In Proceedings of the LDA-Symposium Copenhagen 1975: 64-80, Copenhagen: P.O. Box 70, 1740 Skovlunde, Denmark. 736 pp.

Lumley, J.L. (1970) "Stochastic Tools in Turbulence", Academic Press, New York.

Lumley, J.L. (1957) "Some Problems Connected With the Motion of Small Particles in Turbulent Fluid". PhD. Thesis, The John Hopkins University.

Lumley, J.L. (1976) "Two-phase and Non-Newtonian Flows, in Turbulence". Topics in Applied Physics, Vol. 12; 290-324.

Lumley, J.L., George, W.K. and Buchhave, P. (1978). "Influence of Refractive Index Fluctuation on Velocity Measurements with a Laser Doppler Anemometer". To be submitted for publication, The Physics of Fluids.

Lumley, J.L., Buchhave, P. and George, W.K. (1978) "Influence of Dropout on Velocity Measurements with Continuous Laser Doppler Anemometer. To be submitted for publication, The Physics of Fluids.

Mayo, W.T., Shay, M.T. and Riter, S.(1974). "The Development of New Digital Data Processing Techniques for Turbulence Measurements with a Laser Velocimeter" Final Report (AEDC-TR-74-53), USAF Contract Co. F40600-73-C-003, August, 1974.

Mayo, W.T.,Jr. (1975) "Modeling of Laser Celocimeter Signals as Triply Stochastic Poisson Processes". In Proceedings of the Minnesota Symposium on Laser Doppler, University of Minnesota, Bloomington, MI. Oct. 1975.

Mayo, W.T., Jr. (1977). "Study of Photon Correlation Techniques for Processing of Laser Velocimeter Signals". NASA Report CR-2780, Feb. 1977 (N77 19761): pp. 104.

McLaughlin, D.K. and Tiederman, W.G. (1973) "Biasing Correcting for Individual Realization of Laser Anemometer Measurements in Turbulent Flows". Phys. Fluids 16: 2082-2088.

Monin, A.S. and Yaglom, A.M. (1975) "Statistical Fluid Mechanics", (J.L. Lumley, ed.) Vol. 2. The M.I.T. Press, Cambridge.

Morton, J.B. and Clark, W.H. (1971)"Measurements of Two-point Velocity Correlations in a Pipe Flow Using Laser Anemometers". J. Phys. E, 4: 809-814.

Neubert, J.A. (1970) "Sound Propagation in Continuous Stochastic Media". Ph.D. Thesis, The Pennsylvania State University.

Quigley, M.S. and Tiederman, W.G.,Jr. (1977) "Experimental Evaluation of Sampling Bias in Individual Realization Laser Anemometry". AIHA J., 15: 266-268.

Reed, (1978) Private Communication.

Scott, P.F. (1974) "Theory and Implementation of Laser Velocimeter Turbulence Spectrum Measurements". In Proceedings of the Second International Workshop on Laser Velocimetry, March 27-29, 1974. Purdue University (Bulletin No. 144), W. Lafayette, Ind. 47907.

Shapiro, H.S. and Silverman, R.A. (1960) "Alias-Free Sampling of Random Noise". J. Soc. Indust. Appl. Math. 8: 225-248.

Smith, D.M. and Meadows, D.M. (1974) "Power Spectra from Random-time Samples for Turbulence Measurements with a Laser Velocimeter". In Proceedings of a Second International Workshop on Laser Velocimetry, March 27-29, 1974, Purdue University, W. Lafayette, Ind. 47907.

Tatarski, V.I., (1961) "Wave Propagation in a Turbulent Medium (R.A. Silverman, trans.) Dover Publications Inc., New York.

Tennekes, H. and Lumley, J.L. (1972) "A First Course in Turbulence". M.I.T. Press, Cambridge.

Tiederman, W.G.,Jr. (1977) "Interpretation of Laser Velocimeter Measurements in Turbulent Boundary Layers and Regions of Separation. at Fifth Biennial Symposium on Turbulence, Oct. 3-5, 1977, University of Missouri, Rolla.

Thompson, H.D. and Stevenson, W. H. (eds.) (1974). Proceedings of the Second International Workshop on Laser Velocimetry, March 27-29, 1974. (Bulletin No. 144), Purdue University, W. Lafayette, Ind. 47907.

Townsend, A.A. (1956) "The Structure of Turbulent Shear Flow". Cambridge The University Press.

Van Maanen, H.R.E., Von der Molen, K. and Blom,J.(1976). "Reduction of Ambiguity Noise in Laser Doppler Velocimetry by a Cross Correlation Technique". In Proceedings of the LDA-Symposium Copenhagen 1975: pp. 81-88. Copenhagen: P.O. Bos 70, 1740 Skovlunde, Denmark, 736 pp.

Wang, J.C.F. (1976)"Measurement Accuracy of Flow Velocity Via a Digital Frequency-Counter Laser Velocimeter Processor". In Proceedings of the LDA-Symposium Copenhagen 1975: pp. 150-175. Copenhagen: P.O. Box 70, 1740 Skovlunde, Denmark, 736 pp.

Wilmshurst, T.H. and Rizzo, J.E. (1974) "An Autodyne Frequency Tracker for Laser Doppler Anemometry". J. Phys. E., F: 924-930.

TABLE I

Formulas For Calculating Ambiguity Bandwidths
From Berman and Dunning (1973) and George and Lumley (1973)

Transit Time: $\Delta\omega_L = \bar{u}/\sqrt{2}\sigma_1$

Turbulent: $(\Delta\omega_T)^2 = 2/15 \cdot (\underline{K}\sigma_2)^2 (\varepsilon/\nu)\left[\bar{1} + \sin^2 1/2\theta\left\{\frac{1+2\cos 1/2\theta}{2\cos^2 1/2}\right\}\right]$

Mean Gradient: $\Delta\omega_G = K\sigma_2 (-d\bar{u}/dx_2)$

Total: $(\Delta\omega)^2 = (\Delta\omega_L)^2 + (\Delta\omega_G)^2 + (\Delta\omega_T)^2$

TABLE II

Statistical Properties of Phase Fluctuations

Probability Density - $p_{\dot{\phi}}(x) = 1/2 \left[1 + \frac{x^2}{(\Delta\omega)^2}\right]^{-3/2}$

Autocorrelation - $\overline{\dot{\phi}(t)\,\dot{\phi}(t+\tau)} = 1/2 \left(\frac{d\rho}{d\tau^2} - \rho^2\right) \frac{\ell n\,(1-\rho^2)}{\rho^2}$

$$\rho = \exp\left\{-(\Delta\omega\tau)^2/2\right\}$$

Spectrum - $$S(\omega) = \frac{1}{4\sqrt{\pi}}\,\Delta\omega \sum_{n=1}^{\infty} n^{-3/2} \exp\left\{-\frac{\omega^2}{4n(\Delta\omega)^2}\right\}$$

FIGURE CAPTIONS

1-1 Wave vector diagram showing directions of incident and scattered light and the velocity vector.

1-2 Optical configuration of typical LDA

2-1 Turbulent spectra normalized in Kolmogorov variables showing effect of spatial averaging (reference I)

2-2 Typical transfer function resulting from averaging of turbulent fluctuations across the volume, $\tilde{m} \propto$ (largest scattering volume dimension)$^{-1}$ (reference I)

2-3 Simulated turbulence and LDA outputs from three types of signal processors - a phase lock loop, a zero-crossing detector, and a frequency lock loop.

2-4 Probability density of random phase fluctuations.

2-5 Autocorrelation of random phase fluctuations.

2-6 Spectrum of random phase fluctuations.

2-7 Typical autocorrelations measured in turbulent flow using an LDA. Finite value for $\tau = 0$ reflects effect of finite bandwidth of detector.

2-8 "Velocity" spectra measured in turbulent pipe flow showing effect of phase fluctuations at high frequencies. (Berman and Dunning (1973).

2-9

2-10 Oscilloscope traces showing (from bottom): the Doppler current, LDA output (threshhold at zero) and LDA output (threshhold set to eliminate large phase fluctuations).

3-1 Typical $u_0(t)$ from equation (3.2.1) illustrating how the velocity is sampled by individually arriving particles.

3-2 Computation of the autocorrelation from burst processors using only the overlap times for different particles. The middle trace is the upper trace displaced by amount τ as shown.

3-3 Measuring volume cross-section.

3-4 Measuring volume cross-section as a function of angle in the x-y plane (θ=45°).

3-5 Calculated bias error of mean and rms velocity measurements for 3-D Gaussian, isotropic turbulence including effects of measuring volume cross-section.

FIGURE CAPTIONS

3-6 Velocity probability distribution for uncorrected 2-D velocity fluctuations showing effects of bias and results of McLaughlin-Tiederman correction.

3-8 Mean velocity bias in Poissenille flow (after Kreid 1973).

3-8 Calculated bias error of mean and rms velocity measurement in 3-D Gaussian, isotropic turbulence including effects of measuring volume cross-section.

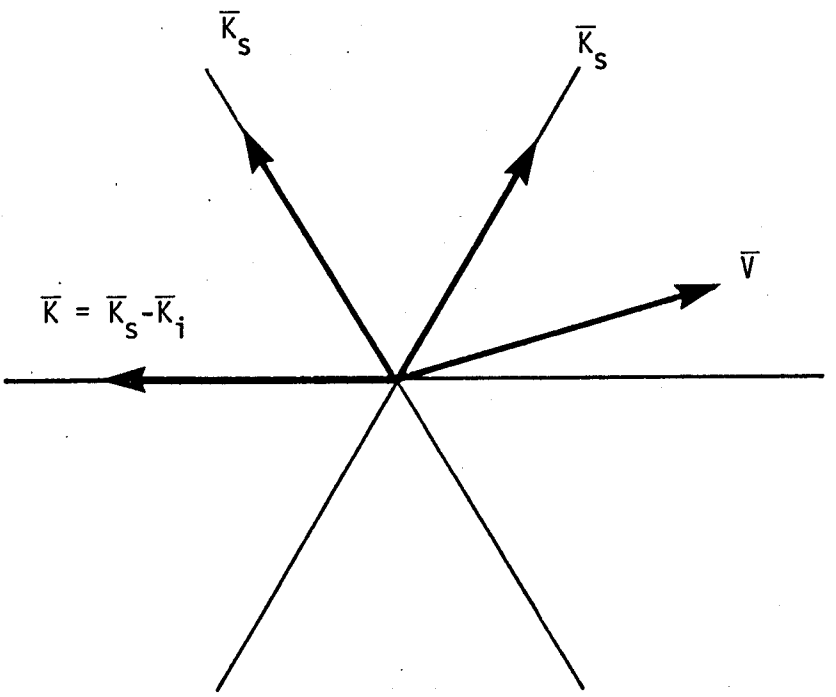

$$\omega_D = \overline{V} \cdot \overline{K}_s - \overline{K}_i$$

Figure 1.1 Wave Vector Diagram

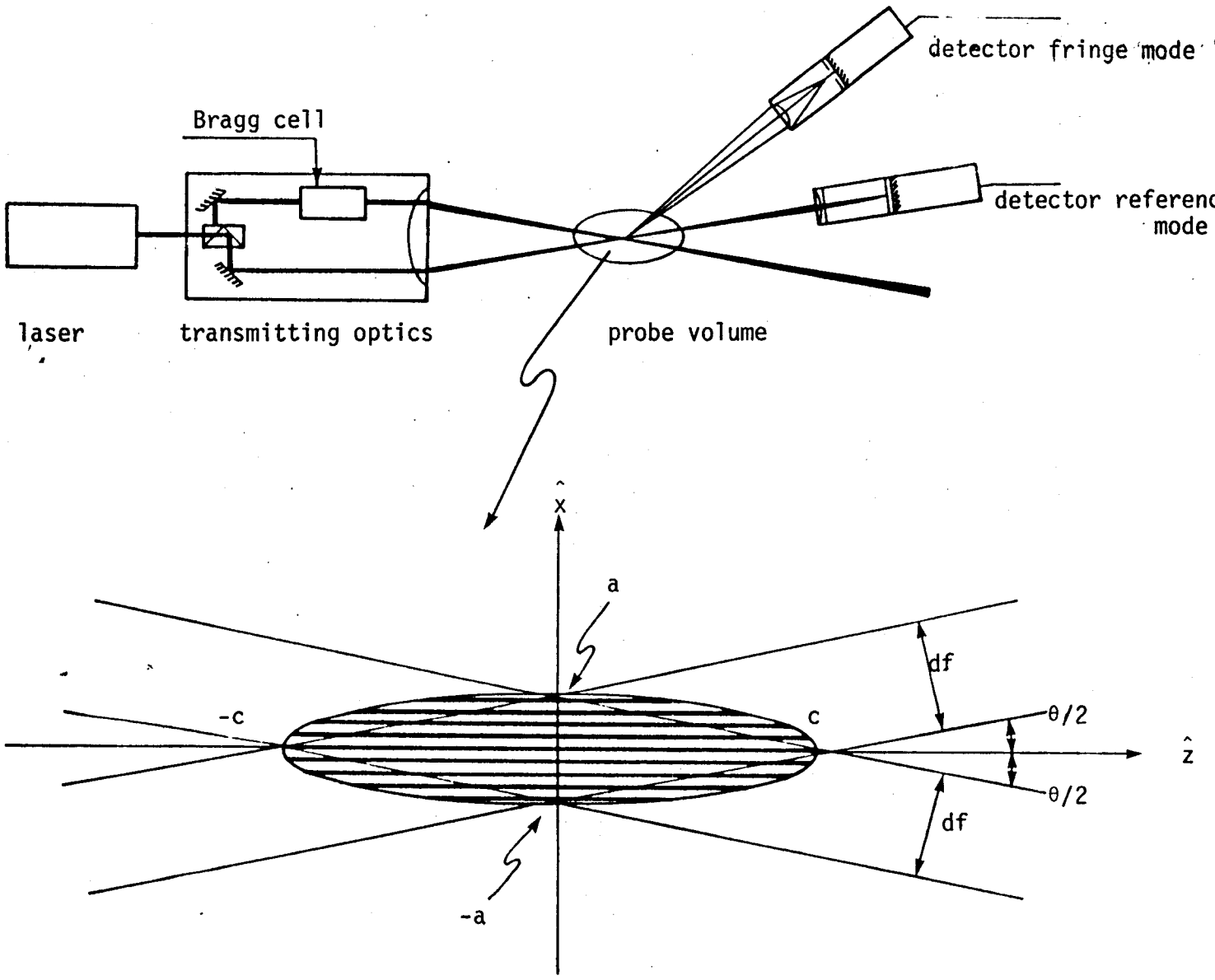

Figure 1.2 Optical Configuration of typical LDA.

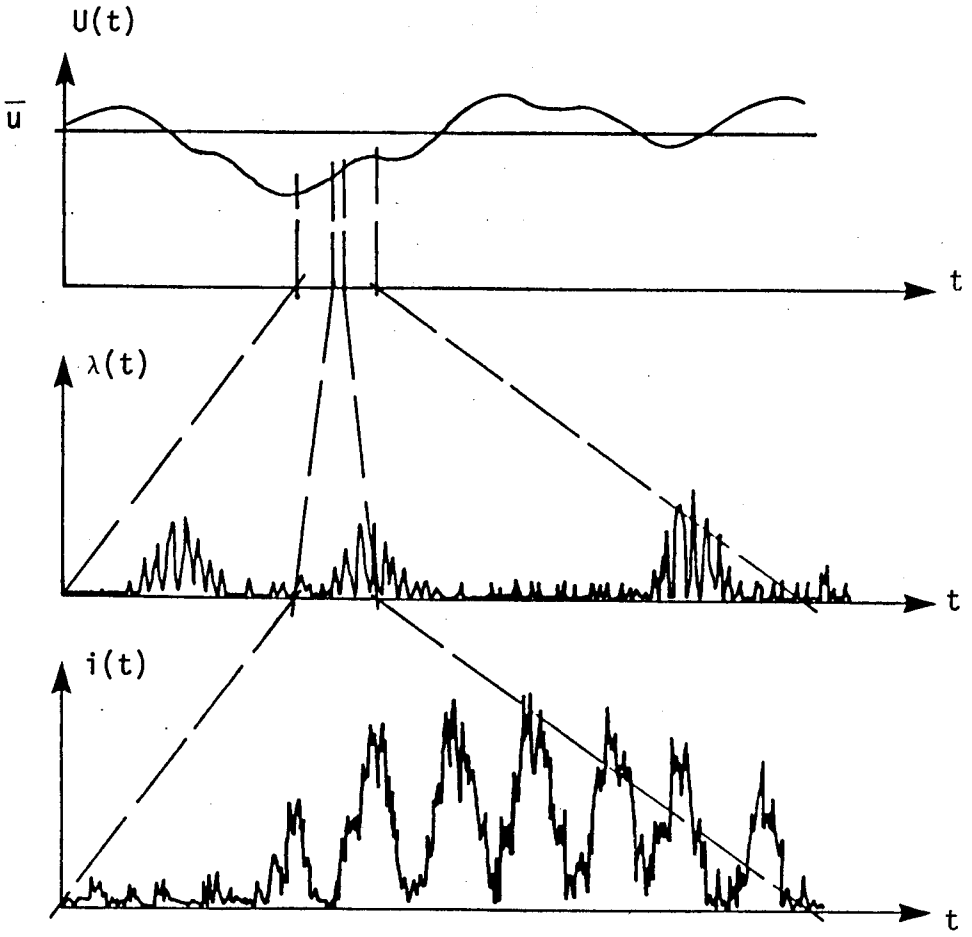

Figure 1.3 Illustration of the stochastic nature of the LDA burst signal (from Mayo 1977).

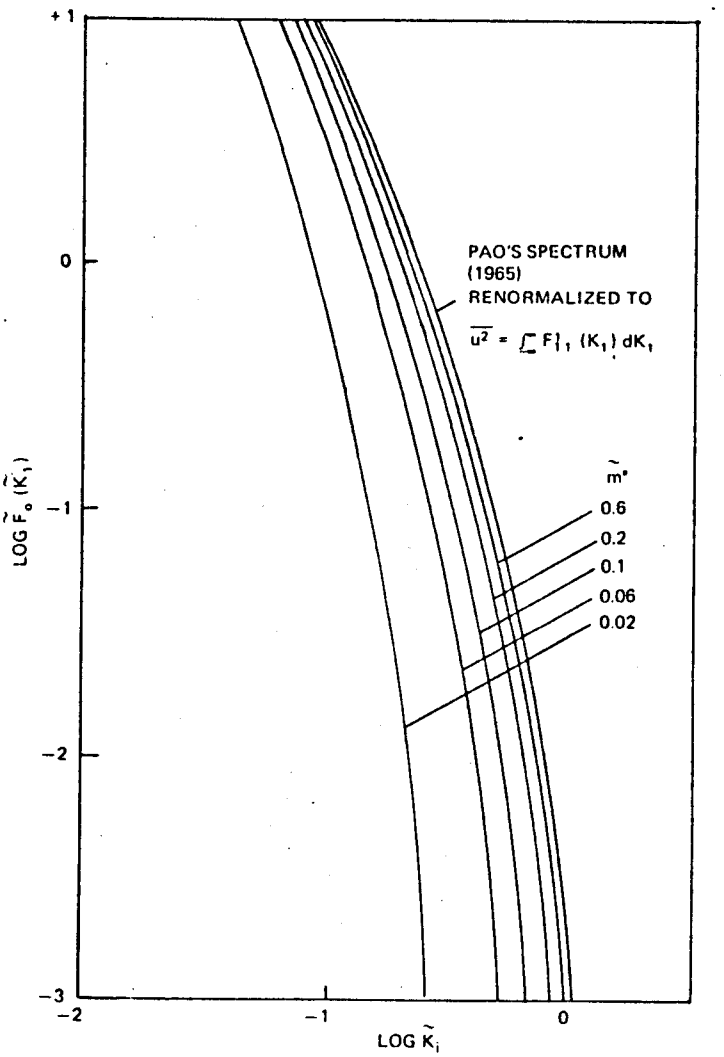

Figure 2.1 Turbulence spectra normalized in Kolmogorov variables showing effect of spatial averaging.

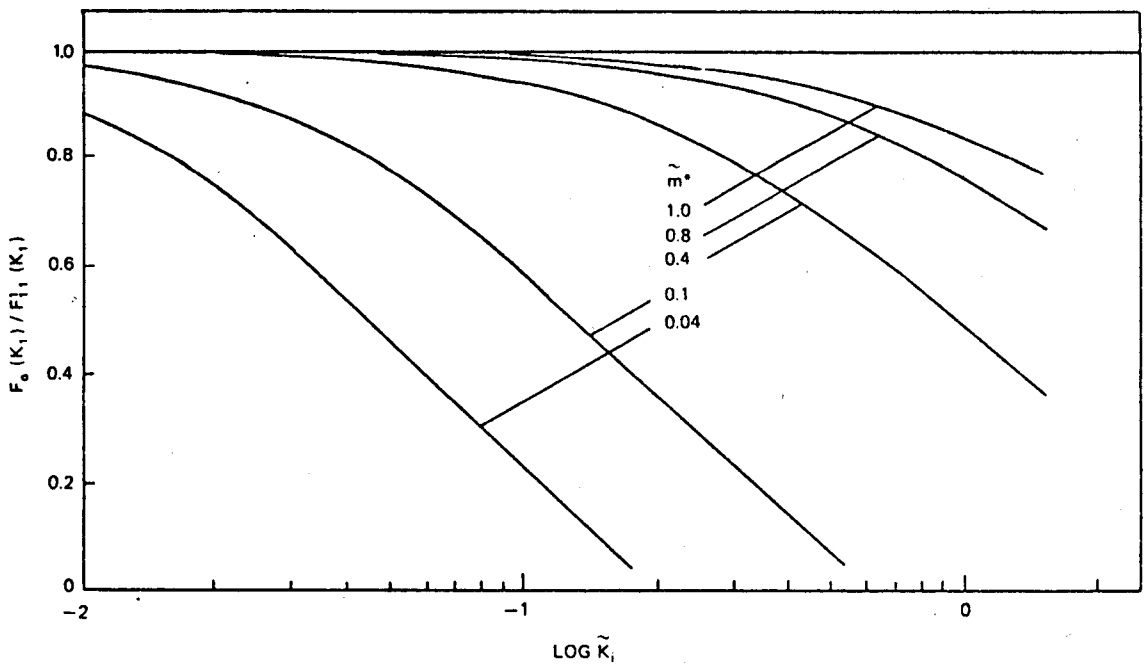

Figure 2.2 Typical transfer function resulting from averaging of turbulent fluctuations across the volume $\tilde{m}_\alpha$ (largest scattering volume dimension) reference 1

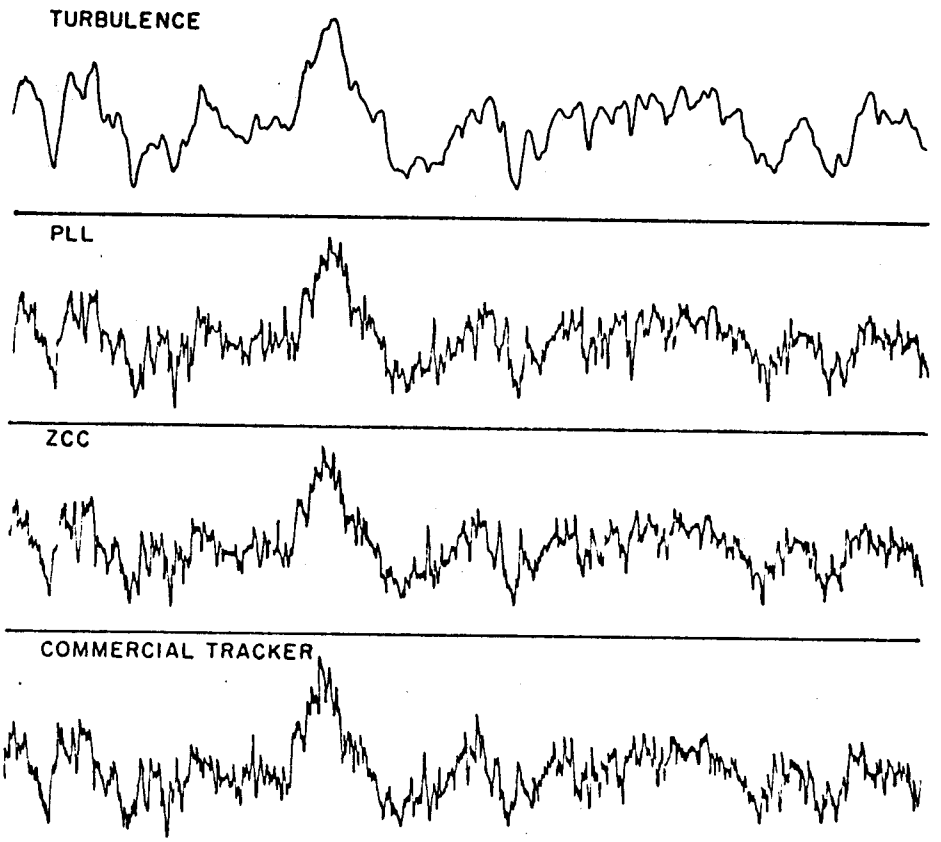

Figure 2-3 Simulated turbulence and LDA outputs from three types of signal processors - a phase lock loop, a zero-crossing detector, and a frequency lock loop.

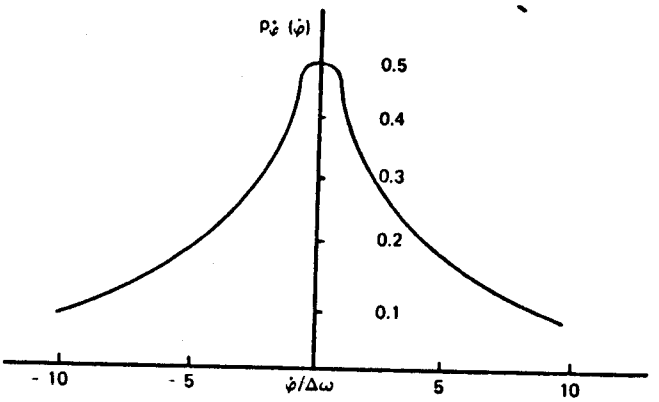

Figure 2-4 Probability density of random phase fluctuations.

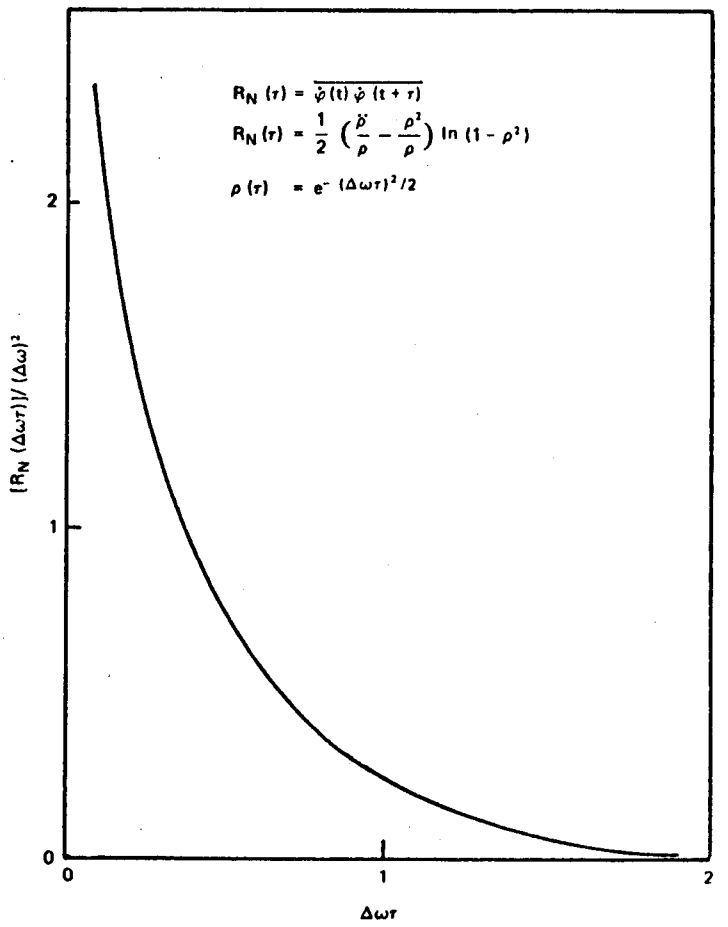

Figure 2-5 Autocorrelation of random phase fluctuations.

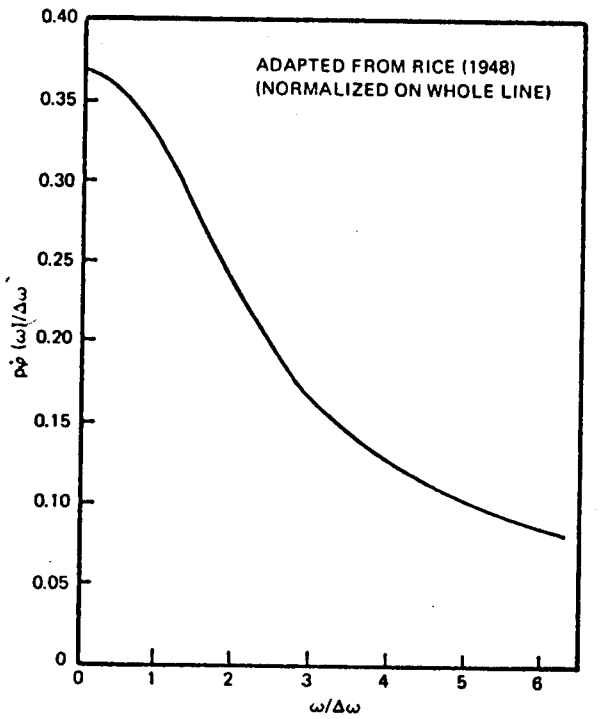

Figure 2-6 Spectrum of random phase fluctuations.

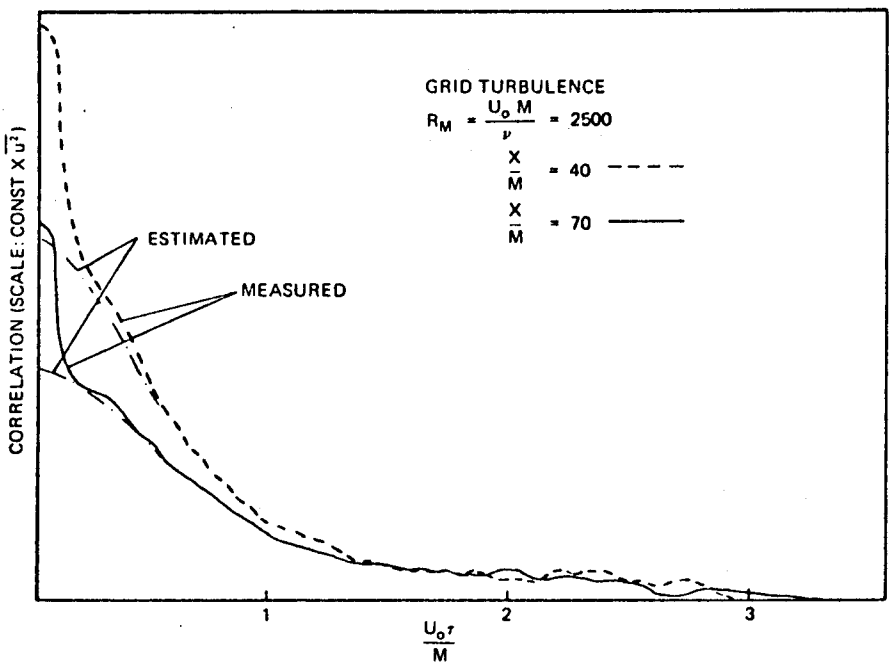

2-7 Typical autocorrelations measured in turbulent flow using an LDA. Finite value for $\tau = 0$ reflects effect of finite bandwidth of detector.

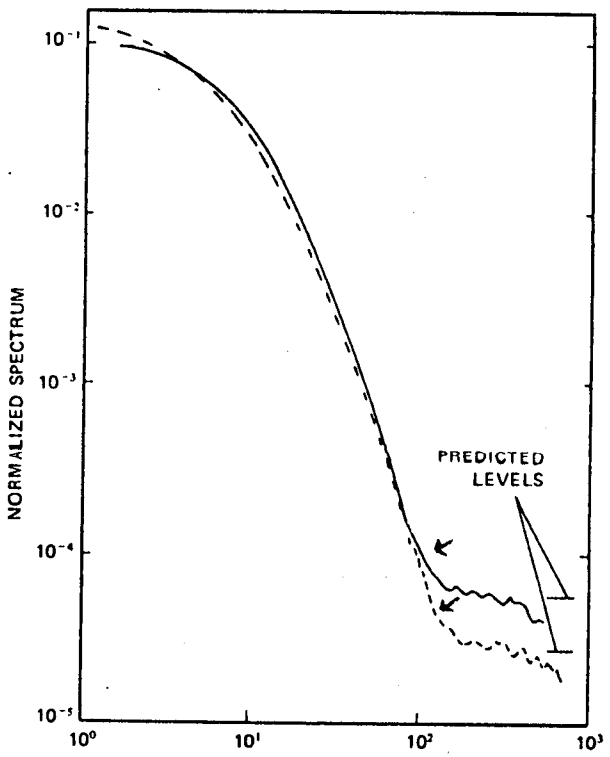

2-8 "Velocity" spectra measured in turbulent pipe flow showing effect of phase fluctuations at high frequencies. (Berman and Dunning (1973)).

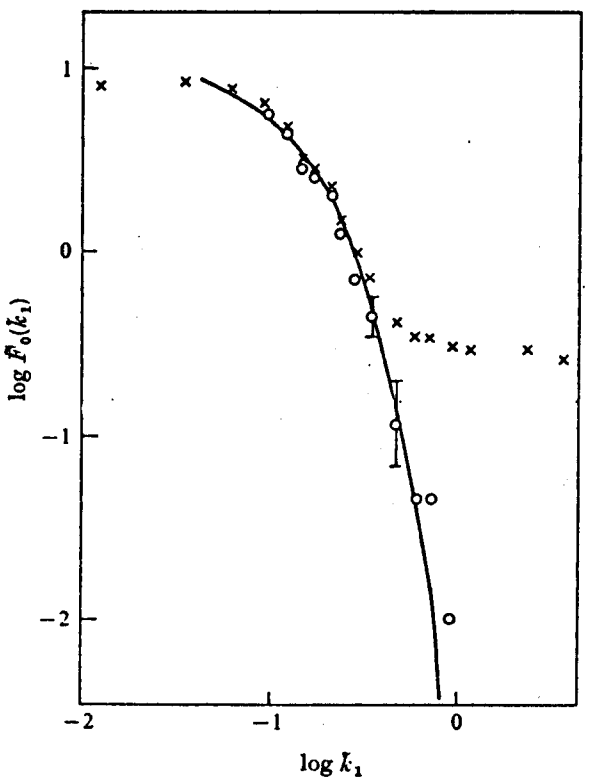

2-9 Turbulence spectrum in grid turbulence · $\frac{X}{M}$ = 45;x-LDA, o-hot film anemometer

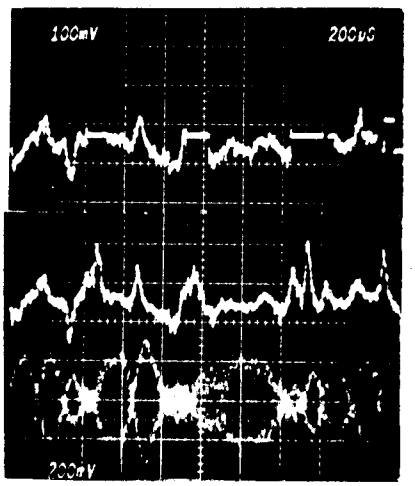

Figure 2-10 Oscilloscope traces showing (from bottom): the Doppler current, LDA output (threshhold at zero) and LDA output (threshhold set to eliminate large phase fluctuations).

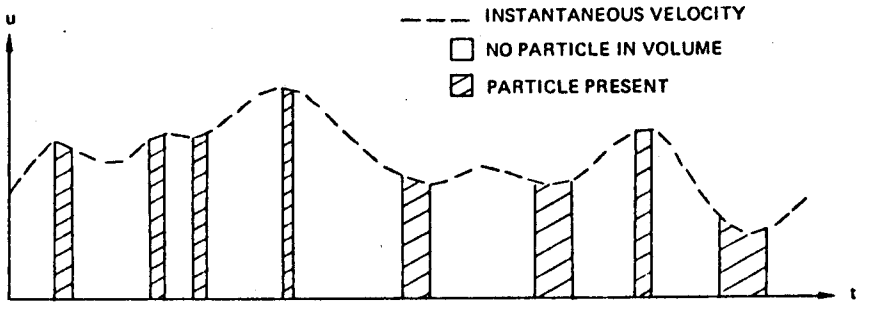

Figure 3-1 Typical $u_o(t)$ from equation (3.2.1) illustrating how the velocity is sampled by individually arriving particles.

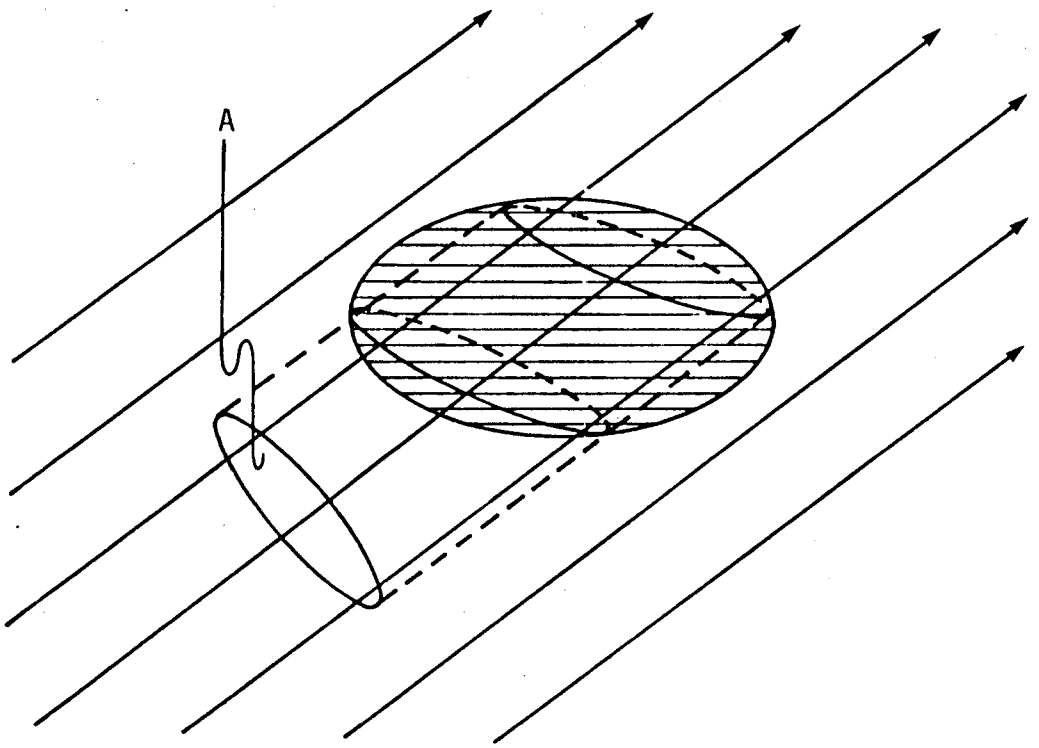

Figure 3-2 Measuring volume cross-section.

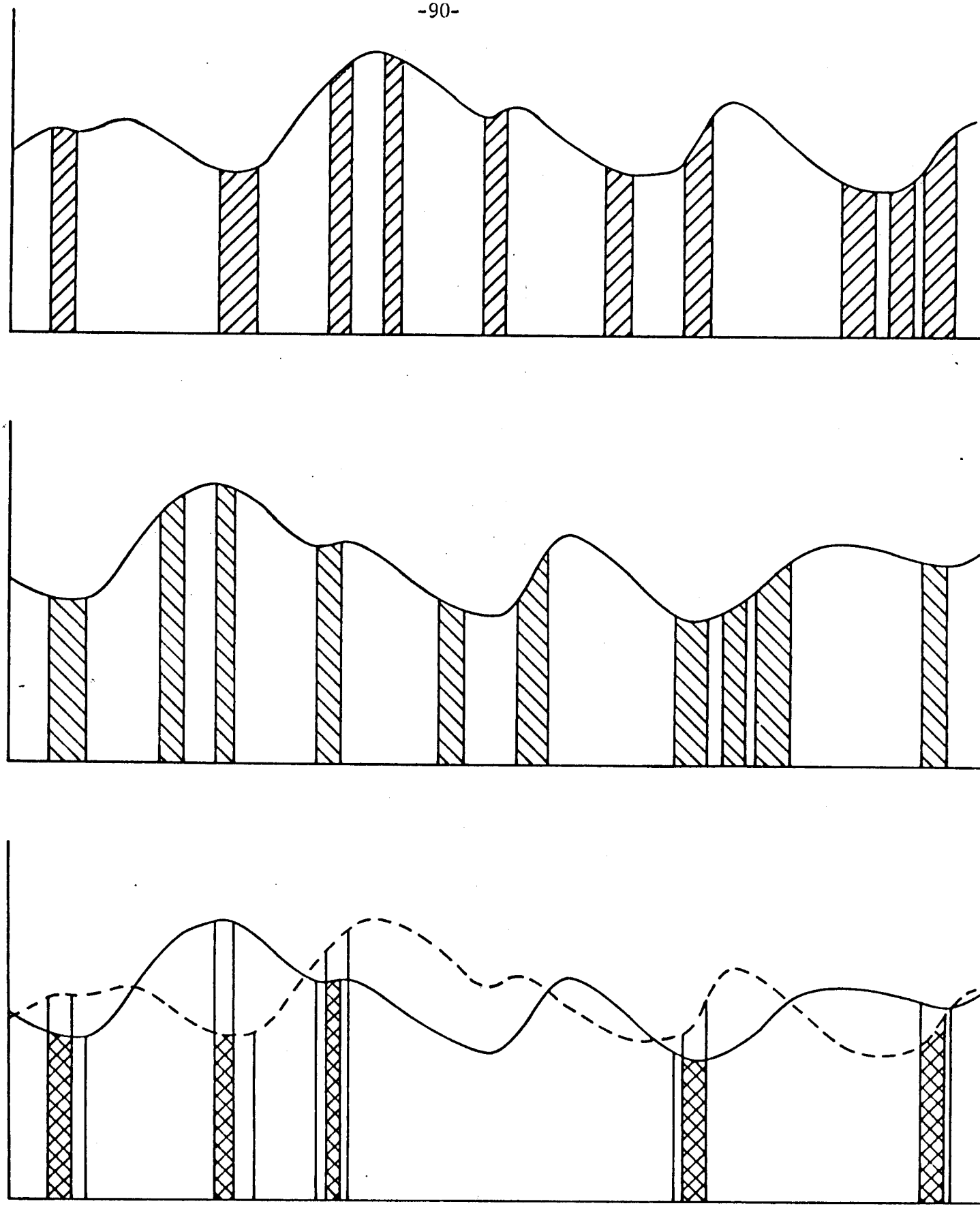

Figure 3-3 Computation of the autocorrelation from burst processors using only the overlap times for different particles. The middle trace is the upper trace displaced by amount τ as shown.

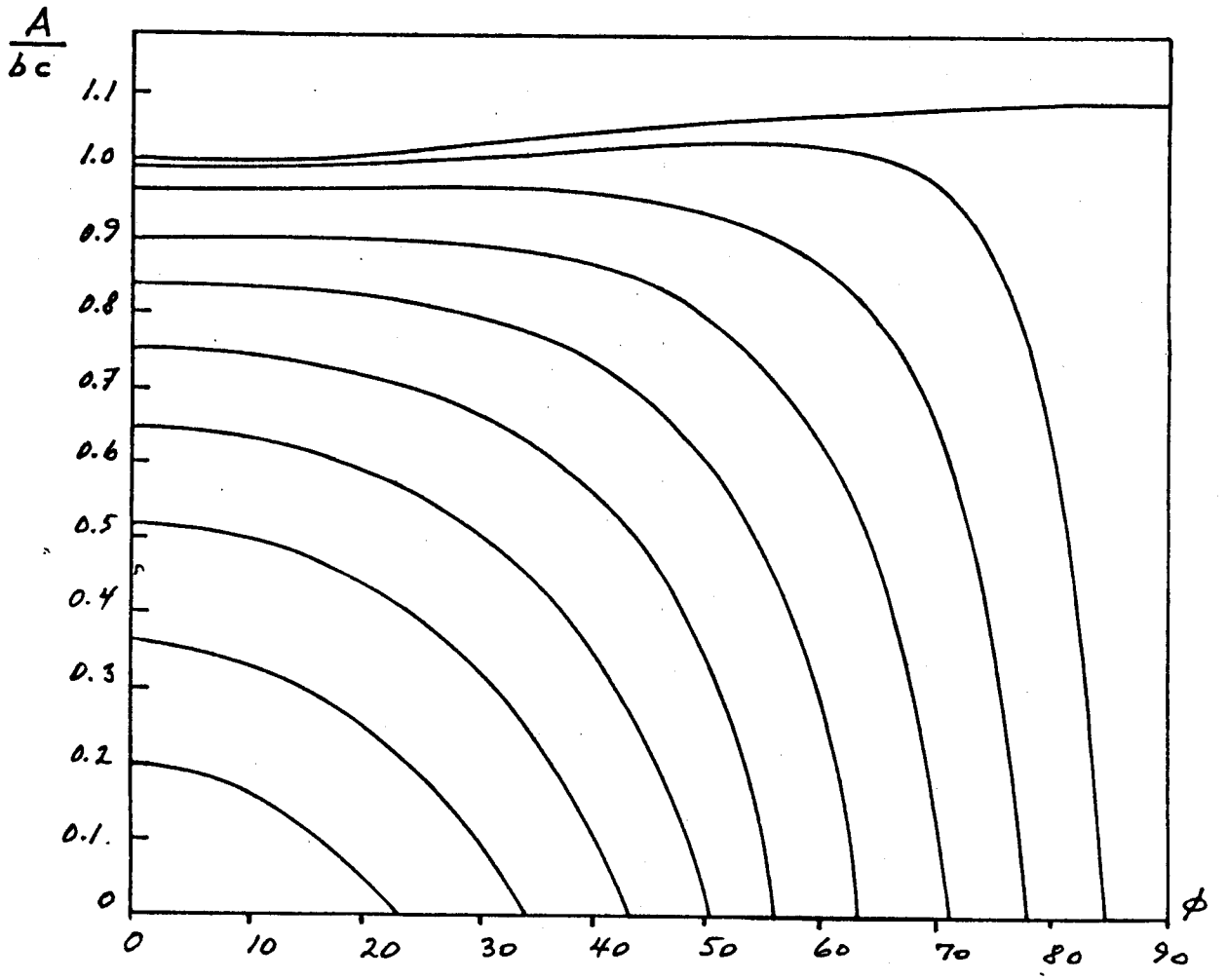

Figure 3-4 Measuring volume cross-section as a function of angle ϕ in the x-y plane (θ=45°).

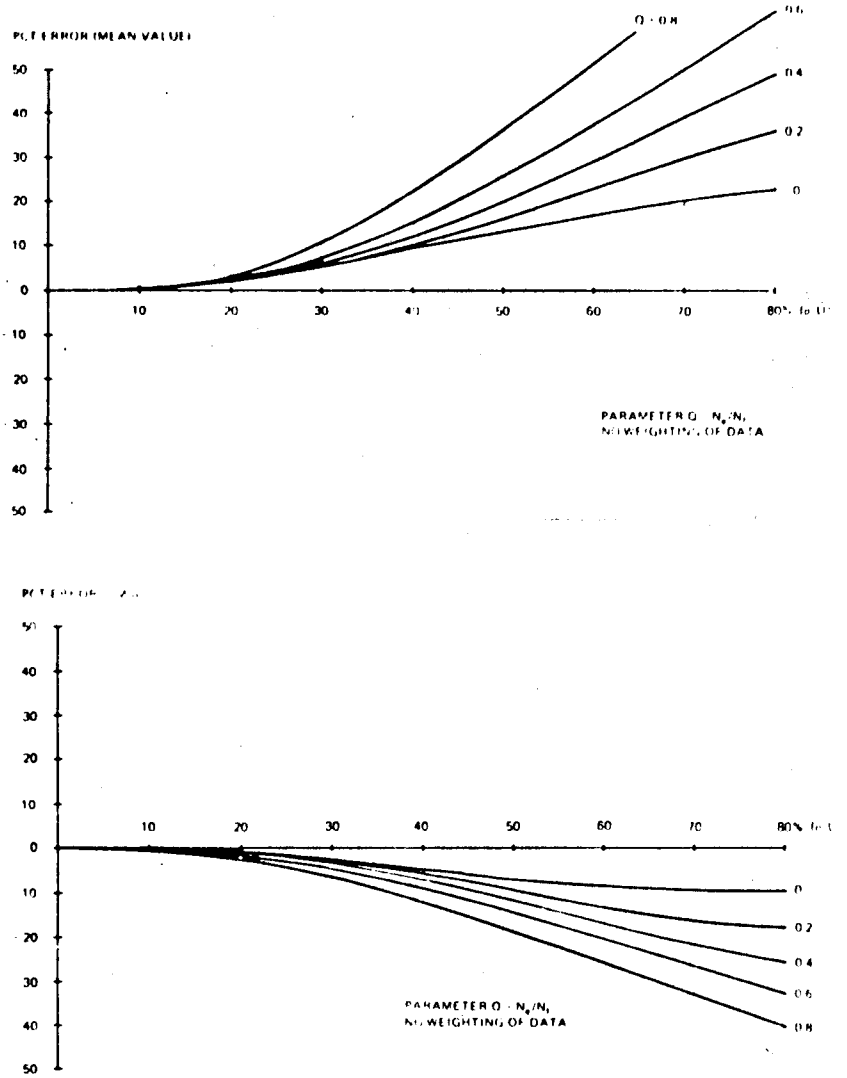

Figure 3-5 Calculated bias error for mean and r.m.s. velocity measurements for 3-D Gaussian, isotropic turbulence including effects of measuring volume cross-section.

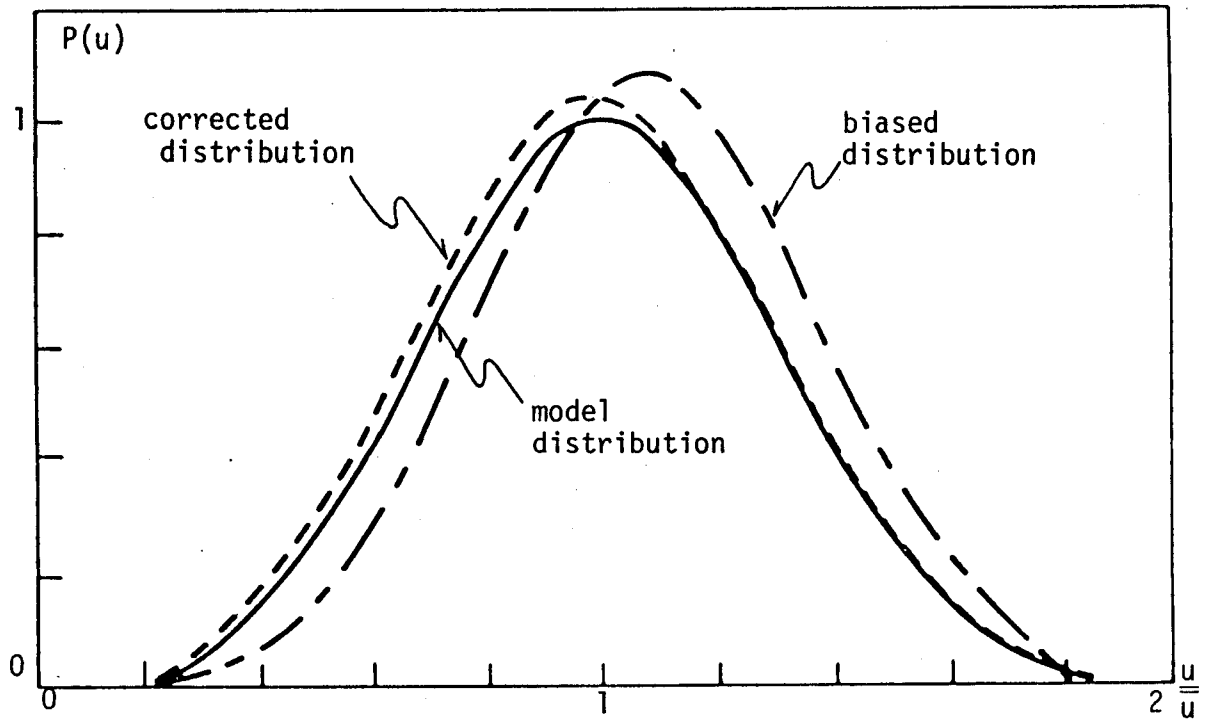

Figure 3-6 Velocity probability distribution for uncorrected 2-D velocity fluctuations showing effects of bias and results of McLaughlin-Tiederman correction.
(after McLaughlin & Tiederman 1973)

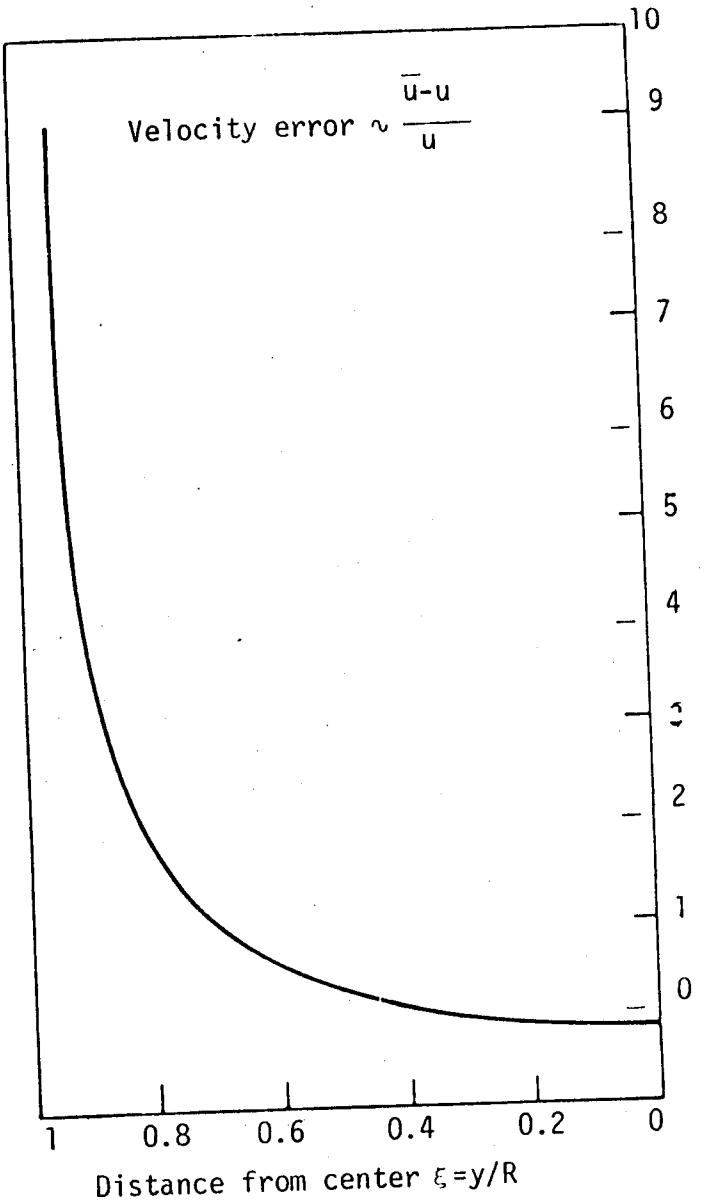

Figure 3-7 Mean velocity bias in Poisseniille flow (after Kreid 1973).

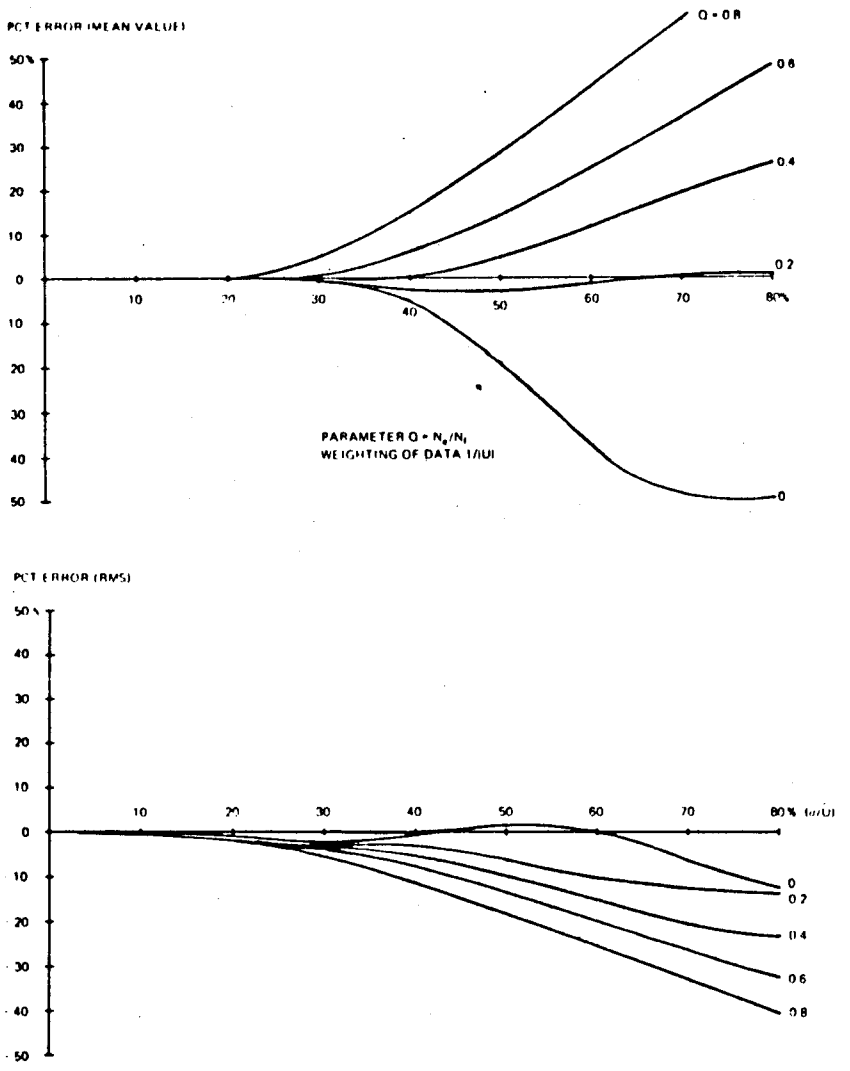

Figure 3-8 Calculated bias error of mean and r.m.s. velocity measurement in 3-D Gaussian, isotropic turbulence including effects of measuring volume cross-section.